

1 An integrated probabilistic assessment to analyze stochasticity
2 of soil erosion in different restoration vegetation

3

4 Ji Zhou ^{1,2,3}, Bojie Fu ^{1,2,*} Guangyao Gao ^{1,2}, Yihe Lü ^{1,2}, Shuai Wang ^{1,2}

5

6

7 ¹ State Key Laboratory of Urban and Regional Ecology, Research Center for Eco-
8 Environmental Science, Chinese Academy of Science, Beijing 100085, PR China,

9 ² Joint Center for Global Change Studies, Beijing 100875, PR China

10 ³ University of Chinese Academy of Sciences, Beijing 100049, PR China

11

12

13 *Corresponding author: Bojie Fu

14 E-mail: bfu@rcees.ac.cn

15 Address: State Key Laboratory of Urban and Regional Ecology, Research Center for
16 Eco-Environmental Science, Chinese Academy of Science, P. O. Box 2871, Beijing
17 100085, PR China

18

19

20

21

22

23 **Abstract:**

24 Stochasticity of soil erosion reflects the variability of soil hydrological response to
25 precipitation under complex environment. Assessing this stochasticity is important to
26 conserve soil and water resources, however stochasticity of erosion event in restoration
27 vegetation types in water-limited environment is less investigated. In this study, we
28 constructed an event-driven framework to quantify the stochasticity of runoff and
29 sediment generation in three typical restoration vegetation types (*Armeniaca sibirica*
30 (T1), *Spiraea pubescens* (T2), and *Artemisia copria* (T3)) at closed runoff plot over five
31 rainy seasons in the Loess Plateau of China. The results indicated that, under the same
32 rainfall condition, the average probabilities of runoff and sediment in T1 (3.8% and
33 1.6%) and T3 (5.6% and 4.4%) were lowest and highest, respectively. The Binomial
34 and Poisson probabilistic model were two effective ways to simulate the frequencies
35 distribution of times of erosion events occurring in all restoration vegetation. The Bayes
36 model indicated that relative longer duration and stronger intensity rainfall events
37 respectively become the main probabilistic contributors of one stochastic erosion event
38 occurring in T1 and T3. Logistic regression modeling highlighted that the higher-grade
39 rainfall intensity and canopy structure were as two most important factors to
40 respectively improve and restrain the probability of stochastic erosion generation in all
41 restoration vegetation types. Bayes, Binomial, Poisson and logistic regression models
42 constituted an integrated probabilistic assessment to systematically simulate and
43 evaluate soil erosion stochasticity. It may be an innovative and important complement
44 in understanding of soil erosion from stochasticity view, and also provide an alternative

45 to assess the efficacy of ecological restoration on conserving soil and water resource in
46 a semi-arid environment.

47

48 **Key words:** stochasticity of soil erosion, Binomial and Poisson, logistic regression
49 model, restoration vegetation,

50

51

52

53

54

55

56

57

58

59

60

61

62

63

64

65

66

67 **1. Introduction**

68 Soil erosion is one of globe environmental problems. In the recent centuries, the erosion
69 rate over worldwide has been accelerating by the climate change and anthropogenic
70 activities, causing soil deterioration and terrestrial ecosystem degradation (Jiao et al.,
71 1999; Marques et al., 2008; Fu et al., 2011; Portenga and Bierman, 2011). The
72 uncertainty and intensity of soil erosion constitute the main feature of erosive
73 phenomenon. Although many studies have been concentrating on the intensity of
74 erosion under different spatiotemporal scales (Cantón et al., 2011; Puigdefàbregas et al.,
75 1999), the uncertainty of soil erosion generation is another challenge of researchers
76 expecting to improve the accuracy of erosion prediction. To some extent, the
77 stochasticity of environment and spatiotemporal heterogeneity of soil loss mainly
78 affected the randomness of runoff production and sediment transportation in natural
79 conditions (Kim. J et al., 2016). Meanwhile, the complex mechanism of erosion
80 generation also increased the uncertainty and variation of erosion processes (Sidorchuk,
81 2005, 2009). Therefore, how to effectively describe the erosive stochasticity and to
82 reasonably assess its impacting factors is necessary and important for understating soil
83 erosion science from the perspective of randomness.

84 First, the combination of various probabilistic, conceptual and physical models have
85 been reported as different integrated approaches to describe the stochasticity of soil
86 erosion intensity (Table 1). As one form of erosion intensity, the runoff processes was
87 proved as a stochastic process by different mathematic simulation models. Some studies
88 (Moore, 2007; Janzen and McDonnell, 2015) have also simulated the stochastic

89 processes, and further quantified the randomness of runoff production and its
90 connectivity dynamics in hillslope and catchment scales by using different probabilistic
91 distribution functions and conceptual models. In these studies, the theory-driven
92 conceptual models simplified main hydrological behaviors related to runoff production,
93 highlighting the stochastic effects of infiltration and precipitation on runoff processes.
94 Based on above precondition, the data-driven probabilistic models further simulated the
95 stochastic runoff production by mapping or calibrating the difference between observed
96 and predicted probabilistic values. As a results, the stochastic-conceptual approaches
97 have formed an effective framework to model the rainfall-runoff processes (Freeze,
98 1980), as well as to assess flood forecasting (Yazdi et al., 2013)

99 The stochasticity of soil erosion rate which is another pattern of erosion intensity was
100 generally investigated by probabilistic and physical models in some studies. The
101 theory-driven physical models in these studies (Sidorchuk, 2005) integrated
102 hydrological and mechanical mechanism of overflow and soil structure with sediment
103 transpiration processes, stressing the stochastic effect of physical principles on erosion
104 rate in different spatial scales (Table 1). Especially Sidorchuk in 2005 further introduced
105 stochastic variables and parameters into probabilistic models by randomizing the
106 physical properties of overflow and soil structure. This approach developed the
107 understanding of uncertainty of sediment transpiration processes, leading the
108 randomness simulation to be better fit the reality of stochastic erosion rate (Sidorchuk,
109 2009). Additionally, the stochasticity of soil erosion rate also reflected the erosion risk
110 which was assessed by the integration of theory-driven empirical model with

111 geostatistics (Jiang et al., 2012; Wang et al., 2002; Kim. J et al., 2016). Erosion risk
112 analysis generally concentrated on the uncertainty or variability of soil erosion rate in
113 catchment and regional scales. It highlighted the impact of the spatiotemporal
114 heterogeneous rainfall and other environment conditions on the stochastic erosion rate.
115 In a word, these probabilistic and physical models constituted a systematical analysis
116 framework which closely related to the principle of water balance and basic
117 hydrological assumptions. It effectively described the randomness of soil erosion rate
118 affected by complex hydrological processes (Bhunya et al., 2007). However, few
119 studies has been made to analyze the stochasticity of soil erosion events. Especially,
120 there are little effort to systematically investigate how the signal of stochastic rainfall
121 is transmitted to erosion event occurring in different restoration vegetation types based
122 on observational data rather than on other model assumptions. In fact, this event-based
123 investigation deriving from specific experiment results probably have more practical
124 meaning for understanding the stochastic interaction between rainfall and erosion
125 events.

126 Secondly, the probabilistic approaches have also been reported as a crucial tool to
127 describe the stochasticity of factors affecting soil erosion rate (Table 1). The
128 randomness of soil water content (Ridolfi et al., 2003), antecedent soil moisture
129 (Castillo et al., 2003), infiltration rate (Wang, P and Tartakovsky 2011) and soil
130 erodibility (Wang et al., 2001) in heterogeneous soil types were all modelled by
131 different probability distribution functions. These stochasticity of soil hydrological
132 characteristics related to erosion rate mainly acted as various roles on impacting the

133 spatiotemporal distribution of erosion rate especially generating in regional or even
134 larger spatial scales. Meanwhile, as the main driving force of soil erosion generation,
135 the uncertainty of rainfall event, to some extent, represents the environment
136 stochasticity (Andres-Domenech et al., 2010). Eagleson in 1978 applied probabilistic-
137 trait models to characterize the stochasticity of rainfall event by using Poisson and
138 Gamma probability distribution functions. The stochastic rainfall distribution in
139 different spatiotemporal scales has also been applied to examine the effect of runoff and
140 sediment yield (Lopes, 1996), to calibrate the runoff-flood hydrological model
141 (Haberlandt and Radtke, 2014), as well as to evaluate the sewer overflow in urban
142 catchment (Andres-Domenech et al., 2010).

143 It has been well recognized the role of spatial distribution of vegetation in controlling
144 the soil erosion rate under different spatiotemporal scales (Wischmeier and Smith, 1978;
145 Puigdefabregas, 2005). How the plants reduce soil erosion rate was also illuminated
146 and interpreted by various physical and empirical models (Liu, 2001; Mallick et al.,
147 2014; Prasannakumar et al., 2011). In theory, Puigdefabregas in 2005 proposed
148 Vegetation-Driven-Spatial-Heterogeneity (VDSH) to explain the relationship between
149 vegetation patterns and erosion fluxes, which improves the understanding of
150 hydrological function of plant on erosion processes. Moreover, Trigger-Transfer-
151 Reserve-Pulse (TTRP) framework proposed by Ludwig in 2005, systematically
152 explored the responses and feedback between vegetation patches and runoff-erosion
153 during whole ecohydrological processes. Theoretically, the stochastic signals of
154 different rainfall events could also be disturbed by the hydrological function of plant,

155 which finally affects the randomness of runoff and sediment events occurring in various
156 vegetation types. However, little effort has been made to explore the effect of different
157 vegetation types on the stochasticity of corresponding soil erosion events. In particular,
158 less approaches have been used to analyze how the properties of rainfall, soil and
159 vegetation impact on the stochastic erosion events through event-based investigation
160 deriving from observational data rather than on theory-based models. Actually, logistic
161 regression modeling (LRM) probably deal with above problems. LRM evaluates the
162 causal effects of categorical variables on dependent variables, and quantifies the
163 probabilistic contribution of influencing factors on the randomness of responsive
164 random events in terms of odds ratio (Hosmer et al., 2013). It could be regarded as
165 another probabilistic model to explore the probability-attribution of influencing factors.
166 However, little literature is available on making LRM to explore the probabilistic
167 attributing of stochastic erosion events under complex environmental conditions.

168 In this study, we hypothesized that the uncertainty of erosive events was also an
169 important property of soil erosion phenomenon, and monitored erosion events
170 generating in three typical restoration vegetation types in runoff plots scale over
171 consecutive five years' rainy seasons. We aim to (1) comprehensively describe the
172 stochasticity of runoff and sediment events in details by using probability theory, and
173 (2) to systematically evaluate the effect of the properties of soil, plant and rainfall on
174 the stochastic erosion events by employing LRM approach. The probabilistic
175 description-attribution approach could constitute an integrated probabilistic assessment
176 based on event-driven probability theory and data-drive experimental observation.

177 Meanwhile, the investigation of stochastic soil erosion events by the integrated
178 assessment may be an innovative and important complement in understanding of soil
179 erosion from stochasticity view, but also could provide an alternative to assess the
180 efficacy of ecological restoration on conserving soil and water resource in a semi-arid
181 environment.

182

183 Table 1

184

185 **2. Method**

186 **2.1 Definition and classification of random events**

187 Each observed stochastic weather condition with different durations in field monitoring
188 period was defined as a random experiment. All possible outcomes of a random
189 experiment constituted a sample space (Ω) defined as a random observational event
190 (short for O event). Two mutually exclusive random event types—random rainfall event
191 (short for I event) and random non-rainfall event (short for C event)—constituted the O
192 event. Precipitation is a necessary condition of runoff generation, and the random runoff
193 production event (short for R event) is a subset of I event. Similarly, R event is also a
194 necessary condition of random sediment migration event (short for S event), which lead
195 to S event be a subset of R event. As a result, O, C, I, R, and S events constituted a
196 random events framework (OCIRS) to reflect the stochasticity of environment in which
197 soil erosion events generation.

198 The random event duration in OCIRS is an important property of stochastic weather

199 conditions. In particular, the duration property of I event was closely related to the
200 transmission of stochastic signals of rainfall into the R and S events. According to the
201 rainfall duration patterns in China (Wei et al., 2007), the time interval between two
202 adjacent individual I events is set to be more than 6 hours, forming the criteria for
203 individual rainfall classification. Meanwhile, based on the observation of random
204 events over five consecutive rainy seasons, we summarized duration property of all I
205 events and further classified them into four mutually exclusive I event types. They were
206 a random extreme long rainfall event type (short for Ie event), a random general long
207 duration rainfall event type (short for Il event), a random spanning rainfall event type
208 (short for Is event) whose duration spans two consecutive days, and a random within
209 rainfall event type (short for Iw event) generated in a day. Additionally, the C event can
210 also be divided into two types at daily scale. They are random non-rainfall event type
211 lasting a whole day (short for Cd event), and random non-rainfall event type whose
212 duration is less than 24 hours (short for Ch event) which is interrupted by I event.

213 Table 2 indicated the physical, probabilistic properties and implications of all random
214 event types in OCIRS. The classification process of all random event types was
215 sketched by figure 1a, the Venn diagram of all random event types in OCIRS was
216 showed in figure 1c. Considering the observed longest duration of Ie event
217 approximating 72 hours, in figure 1b, we summarized a series of random event
218 sequences in terms of different combing patterns of I and C events in every three
219 consecutive days during the whole monitoring period.

220

221

Figure 1

222

Table 2

223

224

225 **2.2 Probabilistic description of erosion event**

226 **2.2.1 Conditional probability of erosion event**

227 In the sample space Ω , for any random event type E in OCIRS, we defined $P(E)$ as the
228 proportion of time that E occurs in terms of relative frequency:

$$229 \quad P(E) = \lim_{n \rightarrow \infty} \frac{n(E)}{n} = p_E, \quad p_E \in [0,1] \quad (1)$$

230 Theoretically, $n(E)$ is the number of times in n outcomes of observed random
231 experiment that the event E occurs. According to the law of total probability (Robert et
232 al., 2013), the probability of R event is defined as:

$$233 \quad P(R) = P(RI) = P(R | \cup_{m=1}^4 I_m) P(\cup_{m=1}^4 I_m) = \sum_{m=1}^4 P(R|I_m) P(I_m) = p_R \quad (2)$$

234 I_m , $m=1, 2, 3$ and 4 represent the I_e, I_l, I_s , and I_w respectively, and $P(R|I_m)$ represents
235 conditional probability that R event occur given that m^{th} I event type has occurred.

236 Similarly, the probability of S event is defined as:

$$237 \quad P(S) = P(SI) = P(S | \cup_{m=1}^4 I_m) P(\cup_{m=1}^4 I_m) = \sum_{m=1}^4 P(S|I_m) P(I_m) = p_S \quad (3)$$

238 Equation (2) and (3) quantify the stochastic soil erosion events by using conditional
239 probability.

240 **2.2.2 Probability distribution functions of erosion event**

241 We defined X, Y as two discrete random variables, representing two real-valued
242 functions defined on the sample space (Ω). Let X, Y denote the numbers of times of R

243 and S events occurrence respectively, and assign the sample space Ω to another random
 244 variable Z. $X(R) = x, Y(S) = y, Z(\Omega) = z, y \leq x \leq z$. x, y, z are integers. The ranges
 245 of X and Y are $R_X = \{all\ x: x = X(R), all\ R \in \Omega\}$ and $R_Y = \{all\ y: y =$
 246 $Y(S), all\ S \in \Omega\}$. The probability of x_i or y_j numbers of times of R or S events can
 247 be quantified by probability mass function (PMF) as follow:

$$248\ pmf_X(x_i) = P[\{R_i: X(R_i) = x_i, x_i \in R_X\}] \quad (4)$$

$$249\ pmf_Y(y_j) = P[\{S_j: Y(S_j) = y_j, y_j \in R_Y\}] \text{ for } i \geq j \quad (5)$$

250 PMF in Equation (4), (5) describe the general expression of probability distribution of
 251 all possible numbers of times of R or S events.

252 The random variables X, Y obey the Binominal distribution with n independent
 253 Bernoulli experiments (Robert et al., 2013). Therefore, the PMF of X, and Y can be
 254 defined as follow:

$$255\ pmf_{Xbin}(x) = P_{Xbin}(X = x) = \begin{cases} \binom{n}{x} p_R^x (1 - p_R)^{n-x} & x = 0, 1, 2, \dots, n \\ 0 & elsewhere \end{cases} \quad (6)$$

$$256\ pmf_{Ybin}(y) = P_{Ybin}(Y = y) = \begin{cases} \binom{n}{y} p_S^y (1 - p_S)^{n-y} & y = 0, 1, 2, \dots, n \\ 0 & elsewhere \end{cases} \quad (7)$$

257 where x and y indicate all possible numbers of times of R and S occurring over n I
 258 events. However, when the Bernoulli experiment is performed infinite independent
 259 times ($n \rightarrow \infty$), the Binomial PMF can be transformed into Poisson PMF (proved by
 260 appendix A), and finally expressed as follow:

$$261\ pmf_{Xpoi}(x) = P_{Xpoi}(X = x) = \begin{cases} \frac{\lambda_R^x e^{-\lambda_R}}{x!} & x = 0, 1, 2, \dots \\ 0 & elsewhere \end{cases} \quad (8)$$

$$262\ pmf_{Ypoi}(y) = P_{Ypoi}(Y = y) = \begin{cases} \frac{\lambda_S^y e^{-\lambda_S}}{y!} & y = 0, 1, 2, \dots \\ 0 & elsewhere \end{cases} \quad (9)$$

263 where the parameter $\lambda_R \approx np_R, \lambda_S \approx np_S$. Equation (6) ~ (9) reflect two PMF models
 264 to simulate the probability distribution of R or S events.

265 **2.3 Probabilistic attribution of erosion events**

266 **2.3.1 Bayes model**

267 Based on the Bayes forumula theroy (Sheldon, 2014), if we want to evaluate how much
 268 the probabilistic contributions of k^{th} type of random rainfall event on one stochastic
 269 runoff or sediment event which has been generated and observed, the Bayes model can
 270 quantify the results as follow:

$$271 \quad P(I_k|R) = \frac{P(I_kR)}{P(R)} = \frac{P(R|I_k)P(I_k)}{\sum_{m=1}^4 P(R|I_m)P(I_m)} \quad (10)$$

$$272 \quad P(I_k|S) = \frac{P(I_kS)}{P(S)} = \frac{P(S|I_k)P(I_k)}{\sum_{m=1}^4 P(S|I_m)P(I_m)} \quad (11)$$

273 In fact, the Bayes model provides an important explanation that how the priori
 274 stochastic information ($P(I_k)$) was modified by the posterior stochastic information
 275 ($P(R)$ or $P(S)$). The application of Bayes model in equation (10) ~ (11) reflects the
 276 feedback of random erosion events on the stochastic rainfall events. It could also be
 277 regarded as one pattern of probabilistic attribution to assess the effect of different
 278 random rainfall events on the uncertainty of soil erosion events without considering the
 279 diversity of restoration vegetation.

280 **2.3.2 Logistic regression model**

281 Firstly, we constructed event-driven logistic function, and defined Y_R and Y_S as two
 282 dichotomous dependent variables. When we denoted 1 or 0 to Y_R and Y_S respectively, it
 283 means that a R and S event has occurred or not occurred. Given Y_R is a dichotomous
 284 dependent variable of R event in linear probability model to be expressed as follow:

$$285 \quad Y_{R_i} = \alpha + \beta_1 x_{1i} + \beta_2 x_{2i} + \cdots + \beta_n x_{ni} + \xi_i = \alpha + \sum_{n=1}^n \beta_n x_{ni} + \xi_i \quad (12)$$

286 Then further transforming equation (12) into conditional probability of R event which

287 has generated in i^{th} observation time as follow:

$$288 \quad P(Y_{R_i} = 1 | \cap_{n=1}^n x_{ni}) = P \left[\left(\alpha + \sum_{n=1}^n \beta_n x_{ni} + \xi_i \right) \geq 0 \right]$$

$$289 \quad = P \left[\xi_i \leq \left(\alpha + \sum_{n=1}^n \beta_n x_{ni} \right) \right]$$

$$290 \quad = F \left(\alpha + \sum_{n=1}^n \beta_n x_{ni} \right) \quad (13)$$

291 α, β are constants, $F(\alpha + \sum_{n=1}^n \beta_n x_{ni})$ is the cumulative distribution function of ξ_i

292 when $\xi_i = \alpha + \sum_{n=1}^n \beta_n x_{ni}$. Equation (12) and (13) quantified the stochasticity of Y_{R_i}

293 depending on the linear combination of n influencing factors x_n and measurement error

294 ξ under i^{th} observation times of stochastic runoff generation.

295 Secondly, assuming the probabilistic distribution of ξ_i satisfies logistic distribution

296 and $P(Y_{R_i} = 1 | \cap_{n=1}^n x_{ni}) = p_i$, then the logistic regression modeling (LRM)

297 expression of $Y_{R_i} = 1$ is deduced as follow:

$$298 \quad p_i = F \left(\alpha + \sum_{n=1}^n \beta_n x_{ni} \right) = \frac{1}{1 + e^{-(\alpha + \sum_{n=1}^n \beta_n x_{ni})}} = \frac{e^{\alpha + \sum_{n=1}^n \beta_n x_{ni}}}{1 + e^{\alpha + \sum_{n=1}^n \beta_n x_{ni}}} \quad (14)$$

299 Correspondingly, the LRM of $Y_{R_i} = 0$ can be express as:

$$300 \quad P(Y_{R_i} = 0 | \cap_{n=1}^n x_{ni}) = 1 - p_i = \frac{1}{1 + e^{\alpha + \sum_{n=1}^n \beta_n x_{ni}}} \quad (15)$$

301 The ratios of equation (14) to (15) is defined as odds of R event:

$$302 \quad \text{Odds} = \frac{p_i}{1 - p_i} = \frac{\frac{e^{\alpha + \sum_{n=1}^n \beta_n x_{ni}}}{1 + e^{\alpha + \sum_{n=1}^n \beta_n x_{ni}}}}{\frac{1}{1 + e^{\alpha + \sum_{n=1}^n \beta_n x_{ni}}}} = e^{\alpha + \sum_{n=1}^n \beta_n x_{ni}}, \quad \text{odds} \in [0, 1] \quad (16)$$

303 In this study, the odds in equation (16) is a probabilistic attribution index to quantify

304 how much the n influencing factors to affect the generation of i^{th} stochastic runoff event.

305 Specifically, when the odds of an influencing factor is greater (less) than 1, it means

306 that the corresponding influencing factor exerts positively (negatively) effects on the
307 probability of R generation.

308 Finally, taking the natural logarithms of the both sides of equation (16), we transform
309 the odds of stochastic runoff event into linear equation (17) reflecting the standard
310 expression of LRM:

$$311 \ln \left[\frac{P(Y_{R_i} = 1 | \cap_{n=1}^n x_{ni})}{P(Y_{R_i} = 0 | \cap_{n=1}^n x_{ni})} \right] = \ln \left(\frac{p_i}{1 - p_i} \right) = \alpha + \sum_{n=1}^n \beta_n x_{ni} \quad (17)$$

312 LRM could be regarded as another probabilistic attribution pattern to evaluate the effect
313 of mutiple impacting factors—such as soil, vegetation, and rainfall—on the randomness
314 of soil erosion events occurring in different restoration vegetation types.

315

316 **3. Experimental design and data analysis**

317 **3.1 Study area**

318 The study was implemented in the Yangjuangou Catchment (36°42'N, 109°31'E, 2.02
319 km²) which is located in the typical hilly-gully region of the Loess Plateau in China
320 (Figure 2a). A semi-arid climate in this area is mainly affected by the North China
321 monsoon. Annual average precipitation reaches approximately 533 mm, and the rainy
322 season here spans from June to September (Liu et al., 2012). The Calcaric Cambisol
323 soil type (FAO-UNESCO, 1974) with weak structure and higher erodibility in the Loess
324 Plateau is vulnerable to water erosion. For these reasons, soil and water loss was one of
325 most environmental problems to seriously degrade the ecosystem in the Loess Plateau
326 before 1980s (Miao et al., 2010; Wang et al., 2015). After that, as a crucial soil and
327 water resource protection project, the Grain-for-Green Project was widely implemented

328 in the Loess Plateau. A large number of steeply sloped croplands were abandoned,
329 restored or natural recovered by local shrub and herbaceous plants (Cao et al., 2009;
330 Jiao et al., 1999). In the Yangjuangou Catchment, the main restoration vegetation
331 distributed on hillslopes includes *Robinia pseudoacacia* Linn, *Lespedeza davurica*,
332 *Aspicilia fruticosa*, *Armeniaca sibirica*, *Spiraea pubescens*, and *Artemisia copria*, etc.
333 All the restoration vegetation was planted over 20 years ago.

334 **3.2 Design and monitoring**

335 In the Yangjuangou Catchment, we have had conducted a systematic long-term field
336 experiments, including the monitoring of soil erosion (Liu et al., 2012; Zhou et al.,
337 2016), observation of soil moisture dynamic (Wang et al., 2013; Zhou et al., 2015) and
338 assessment of soil controlling service in this typical water-restricted environment (Fu
339 et al., 2011).

340 In this study, we first monitored the soil erosion events occurring in three typical
341 restoration vegetation (*Armeniaca sibirica* (T1), *Spiraea pubescens* (T2) and *Artemisia*
342 *copria* (T3)) from rainy season of 2008 to 2012 (figure 2b). Each restoration vegetation
343 type was designed in three 3 m by 10 m closed runoff-plot distributing on southwest
344 facing hillslopes with a 26.8% aspect. The boundaries of each runoff-plot were
345 perpendicularly fenced by impervious polyvinylchloride (PVC) sheet with 50 cm depth.
346 Collection troughs and storage buckets were installed at the bottom boundary to collect
347 the runoff and sediment (Zhou et al., 2016). Under natural precipitation condition, we
348 recorded the number of times of stochastic runoff and sediment events generating in
349 each runoff-plot over five rainy seasons. Meanwhile, we collected runoff and sediment,

350 and separated them after settling the collecting bottles for 24 hours, dried at 105 °C over
351 8 hours and weighted.

352 Secondly, we systematically monitored the hydrological properties of soil in different
353 restoration vegetation types. In the rainy season of 2010, the dynamic of soil moisture
354 was started to be measured in the study region (Wang et al., 2013). The real-time
355 dynamic data of soil water content with interval of 10 minutes were recorded by the S-
356 SMC-M005 soil moisture probes (Decagon Devices Inc., Pullman, WA), and were
357 collected by HOBO weather station logger (figure 2c). These data provided the
358 information about average antecedent soil moisture (short for ASM) before every
359 rainfall events generating in the two rainy seasons from 2010 to 2012. We further
360 measured the field saturated hydraulic conductivity (short for SHC) in all vegetation
361 types by Model 2800 K1 Guelph Permeameter (Soilmoisture Equipment Corp., Santa
362 Barbara, CA, USA) to determine the average infiltration capability of soil matrix (figure
363 2d).

364 Thirdly, we also investigated the morphological properties of different vegetation
365 types in each runoff-plot for 2-3 times over different periods of rainy season. We
366 measured the average crown width, height and the thickness of litter layer in three
367 restoration vegetation by setting 60 × 60 cm quadrats in each runoff plot (Bonham, 1989)
368 (figure 2e).

369 Finally, two tipping bucket rain gauges were installed outside of runoff-plot to
370 automatically record the rainfall processes over the five rainy seasons with an accuracy
371 of 0.2 mm precipitation. Table 3 summarized the properties of four types of random

372 rainfall event, and all the basic characteristic of soil and vegetation was showed in Table
373 4.

374 Figure 2

375 Table 3

376 Table 4

377

378 **3.3 Statistics**

379 We employed nonparametric statistical tests—one-way ANOVA and post hoc LSD—to
380 determine the significant difference of soil, vegetation and erosive properties in the
381 three restoration vegetation types. meanwhile, the maximum likelihood estimator (MLE)
382 and uniformly minimum variance unbiased estimator (UMVUE) (Robert et al., 2013)
383 were explored to compare the suitability of the binomial PMF and Poisson PMF for
384 predicting the uncertainty of runoff and sediment generation over long term.

385

386 **4. Results**

387 **4.1 Environmental stochasticity in different rainy seasons**

388 The probabilistic distribution of random rainfall events (I events) and random non-
389 rainfall events (C events) forms the environmental stochasticity which is a background
390 of stochastic soil erosion generation. In the OCIRS, the stochastic environment at
391 monthly and seasonal scales over five rainy seasons was described by figure 3. From
392 the rainy season of 2008 to 2012, the probability of I event generation firstly increased
393 with the increasing of monitoring period and then decreased in the last two rainy

394 seasons. In the rainy season of 2008, the average probability of I event was lower than
395 other four rainy seasons, with being less than 15%. However, the types of I events was
396 most complex in 2008. The random extreme long rainfall event (Ie event) only appeared
397 in this rainy season, with the probability even reaching to 2.5% On the other hand, the
398 average probability of I event was the highest in the rainy season of 2010, with being
399 larger than 18%. But, there only existed two types of I events (Iw and Is events) in this
400 rainy season. Over the five rainy seasons, the average probability of Iw (12.3%) and Ie
401 (0.8%) events generation were the highest and lowest, respectively. The average
402 probability of Is (1.7%) and II (1.3%) events ranged between Iw and Ie. The probability
403 of Cd event was higher than Ch in each month of rainy season, with average probability
404 being 54.4% and 29.4%, respectively. Moreover, in the table 3, the difference of average
405 precipitation and duration in the four types of I events was significance. But the average
406 rainfall intensity of Iw and Is events were nearly twice that of II and Ie events.

407

408 Figure 3

409

410 **4.2 Stochasticity of soil erosion events**

411 **4.2.1 Probability of erosion events in vegetation types**

412 The stochasticity of erosion events was quantified by the probability of runoff and
413 sediment generation in three restoration vegetation types (T1, T2 and T3) under
414 monthly and rainy season scales (figure 4). Over the five rainy seasons, the probability
415 of soil erosion occurring in all vegetation types generally decreased with the increasing

416 of monitoring period, and then increased in 2012. At early period of erosion monitoring
417 (2008), the randomness of erosion events is similar, and the probability of R and S event
418 ranged from 6% to 13% and from 3% to 13% respectively. After that, from rainy season
419 of 2009 to 2011, the highest probabilities of erosion events in each vegetation type all
420 concentrated in the July and August of each season. As to runoff production, the average
421 probability of R event in T1 (3.78%) was less than that of T2 (5.60%) and T3 (5.58%)
422 under same precipitation condition. With respect to sediment yield, the average
423 probability of S event in T1 (1.65%) was also the lowest in all restoration vegetation
424 types. Especially, in the last two rainy seasons, there was no S event occurring in T1,
425 but, the average probability of S event in T2 and T3 reached to 1.83% and 3.36%
426 respectively in corresponding rainy seasons. Consequently, affected by the same
427 stochastic signal of rainfall events, T1 and T3 have the lowest and highest probability
428 of erosion event generation over the five rainy seasons respectively.

429

430 Figure 4

431

432 **4.2.2 Probabilistic distribution of erosion events in vegetation types**

433 More detailed stochastic information of erosion events in different vegetation types was
434 simulated by Binominal and Poisson mass functions (PMFs) under the monthly scales.
435 It also compared the frequencies distribution of different numbers of observed erosion
436 events with the corresponding simulated results by the two PMFs in figure 5. Firstly, as
437 to the detailed stochastic information of R events, the two PMFs generally provided a

438 better simulation to the observation in T1 than that of in T2 and T3. When comparing
439 the simulated and observed values, Binomial PMF supplied better simulation to the
440 observed numbers of time of R events with larger frequency (such as 2~4 time) than
441 that of Poisson PMF. However, Poisson PMF simulated the observed numbers of time
442 of R events with the lower frequency (such as 6~8 times) better than that of Binomial
443 PMFs. Secondly, as to the detailed stochastic information of S event, the two PMFs
444 provided better simulation to the observation in T3 than that of in T1 and T2. In
445 particular, when the number of times of S event generation reaches two in T1 and T2,
446 the corresponding simulated probability values were all nearly 2 times larger than the
447 observed frequencies, reflecting the most simulation error of the two PMFs. Moreover,
448 with the restoration vegetation types changing from T1 to T3, both of the simulated and
449 observed numbers of time of R and S events with largest probability or frequency
450 increased in consistence. In a word, comparing with the observed frequency of numbers
451 of erosion events, both PMFs indicated well-simulating effect to detail the stochasticity
452 of runoff and sediment events under monthly scale.

453

454 Figure 5

455

456 **4.3 Stochastic attribution of soil erosion events**

457 **4.3.1 Effect evaluation of stochastic erosion events by Bayes model**

458 The Bayes model was applied to analyze the effect of random rainfall events (including
459 Iw, Is, Il and Ie) on stochastic erosion events in different restoration vegetation types.

460 Specifically, Bayes model evaluated the different probabilistic contributions of four
461 types of I events on one observed erosion event which has stochastically generated in
462 specific vegetation type under monthly and rainy seasonal scales (figure 6). In the rainy
463 season of 2008, the types of I events driving one stochastic erosion event was most
464 complex than other rainy seasons. In contrast, one stochastic soil erosion generation in
465 three vegetation types attributed to only Iw and Is events in the rainy season of 2010.
466 In other three rainy seasons, when one R or S event stochastically generated on T1, the
467 main contributing I event types concentrated on Is and Ii events both of which have
468 relatively higher precipitation and longer duration, respectively. On the other hand, if
469 one R or S event occurred in T2 or T3 randomly, the main contributing I event types
470 was Iw event which, however, have no contribution to S event occurred on T1.

471 In general, over five rainy seasons, the composition of I event driving one R event
472 was more complex than that of driving one S event. The relative longer duration rainfall
473 events (Ii and Ie) became the main probabilistic contributors of one stochastic erosion
474 event occurring in T1, and the relative stronger intensity rainfall events (Iw and Is)
475 mainly caused one random erosion event generating in T2 and T3.

476

477 Figure 6

478

479 **4.3.2 Effect evaluation of stochastic erosion events by LRM**

480 According to the results of significant difference analysis in table 4, we defined the
481 properties of soil and plant as ordinal variables, and classified them into four grades

482 (Table 5). Meanwhile, based on previous studies (Liu et al., 2012; Wei et al., 2007) and
483 rainfall properties in this study area, we further subdivided all precipitation and rainfall
484 intensity into four grades with different scores.

485 First, the intensity of positive and negative effects of single influencing factor on the
486 probability of runoff and sediment generation in all restoration vegetation types was
487 quantified in terms of odds ratio of erosion events by LRM (table 6). In the LRM, the
488 highest and lowest odd ration appeared in rainfall intensity ordinal variable (INT) and
489 average crown width ordinal variable (CRO). The increasing INT and CRO (from
490 middle to extreme grade) significantly increased and decreased the odds ratio of erosion
491 events, respectively. This means that INT and CRO acts as two most important roles on
492 improving and restraining the probability of stochastic erosion generation in all
493 restoration vegetation types. Additionally, the increasing of antecedent soil moisture
494 ordinal variable (ASM) and the filed saturated hydraulic conductivity ordinal variable
495 (SHC) (from middle to high grade) in the LRM, also significantly increased and
496 decreased the odds ratio of R and S events, respectively. However, the average thickness
497 of litter layers ordinal variable (TLL) has not exerted significant effect on the odds ratio
498 of erosion events. Table S-1 and S-2 in supplementary information systematically
499 describe the whole processes of LRM to evaluate the effect of single factor on odds
500 ratio of erosion event.

501 Secondly, we further applied LRM to evaluate the interactive effects of multiple
502 influencing factors on the odds ratio of R and S events in all restoration vegetation types
503 (table 7). As to the interactive effect of two soil hydrological properties, the interaction

504 between low-grade of SHC and increasing-grade of ASM significantly raised the odds
505 ratio of erosion events. Such that the odds ratio of R and S events affected by the
506 interactive effects of low-grade of SHC and extreme-grade of ASM were respectively
507 7.02 and 1.82 times larger than that interactive effects of low-grade of SHC and low-
508 grade of ASM. Similarly, as to the effect of two vegetation properties, the interactive
509 effect of low-grade of CRO and increasing-grade of TLL would reduce the odds ratio
510 of erosion events. Such that the odds ratio of R and S events influenced by the
511 interaction between low-grade of CRO and high-grade of TLL were respectively only
512 0.12 and 0.33 times larger than that interactive effects of low-grade of CRO and low-
513 grade of TLL. Additionally, with respect to the interaction between soil and plant
514 properties, the interactive effect of low-grade of CRO and increasing-grade of ASM
515 properties also significantly raised the odds ratio of erosion events. The whole processes
516 of LRM to evaluate the interactive effect of multiple factors on odds ratio of erosion
517 event were indicated by the table S-3,4 and 5 in the supplementary information.

518

519

Table 5

520

Table 6

521

Table 7

522

Table S-1,2,3,4,5

523

524

525

526 **5. Discussion**

527 **5.1 The integrated probabilistic assessment to erosion stochasticity**

528 The probabilistic attribution and description of stochastic erosion events constituted the
529 framework of integrated probabilistic assessment (IPA).

530 First, as to one pattern of probabilistic attribution in the IPA, Bayes model supplies a
531 supplementary view and algorithm about how to evaluate the feedback of a result which
532 had stochastically occurred on all possible reasons (Wei and Zhang, 2013). Under the
533 conditions of insufficient information about an occurred result, Bayes model can
534 determine which reasons have the relative greater probability to trigger the occurrence
535 of the result through some prior information. Specific to this study, Bayes model was
536 used to evaluate the probabilistic contribution of four types of I events on one stochastic
537 R ($P(I_k|R)$) and S ($P(I_k|S)$) event generated in each restoration vegetation. Although
538 there were no more specific information about a stochastic soil erosion event, the prior
539 information ($P(R|I_m), P(S|I_m), P(I_m)$) can provide assistance for us to assess the
540 feedback of the stochasticity of soil erosion on different random rainfall events by
541 Bayes model. Meanwhile, ($P(I_k|R)$) and ($P(I_k|S)$) also reflect the different probability
542 threshold values of four rainfall event types triggering soil erosion. Bayes model
543 integrated with total probability theory to systematically quantify the interactive
544 relationship between the stochasticity of precipitation and soil erosion, forming a
545 relative simple and practicable risk assessment of soil erosion event occurring in
546 complex restoration vegetation conditions.

547 Secondly, as a pattern of probabilistic description in the IPA, Binomial and Poisson

548 PMFs are two crucial probabilistic functions to characterize many random hydrological
549 phenomena and to model their ecohydrological effects in natural condition (Eagleson,
550 1978, Rodriguez-Iturbe et al, 1999, 2001). In this study, the two PMFs were found to
551 have good simulations of the frequency of times of soil erosion events in three
552 restoration vegetation types. However, it is necessary and meaningful for the reliability
553 and accuracy of the IPA to assume whether the two PMFs can both stably and
554 reasonably simulate the erosion stochasticity at closed-runoff-plot over longer
555 monitoring period. Therefore, based on above assumption, two important point
556 estimations methods—the maximum likelihood estimator (MLE) and uniformly
557 minimum variance unbiased estimator (UMVUE) (Robert et al., 2013)—were applied
558 to evaluate the stability of erosion stochasticity estimation by means of analyzing the
559 unbiasedness and consistency of p_R, p_S, λ_R and λ_S . Taking parameter analysis of
560 random runoff event for example, we defined X_i as the number of times of R event
561 occurring in some specific restoration vegetation in i^{th} rainy season ($i = 1, 2, 3, 4$ and 5).
562 The five independent and identical (*iid*) random variables satisfies the same and
563 mutually independent binomial or Poisson PMFs as follows:

$$564 \quad X_1, X_2, \dots, X_5 \xrightarrow{iid} \text{binomial}(p_R) \text{ or } X_1, X_2, \dots, X_5 \xrightarrow{iid} \text{Poisson}(\lambda_R) \quad (18)$$

565 Considering longer monitoring periods, we supposed that the numbers of corresponding
566 I events (n) and rainy seasons (i) would approach infinity ($n, i \rightarrow \infty$), and (18) can be
567 transformed as follow:

$$568 \quad X_1, X_2, \dots, X_i \xrightarrow{iid} \text{binomial}(p) \text{ or } X_1, X_2, \dots, X_i \xrightarrow{iid} \text{Poisson}(\lambda) \quad (19)$$

569 We take MLE and UMVUE methods to search for the best reasonable population

570 estimators \hat{p} and $\hat{\lambda}$ to approximate the unknown p and λ in (19), and finally obtain
571 more comprehensive stochastic information about the randomness of R event over i
572 rainy seasons. The Appendix B proved that the best estimator \hat{p} in Binomial PMF is
573 the unbiasedness and consistency of the MLE of p . However, proved by the Appendix
574 C, the best estimator $\hat{\lambda}$ in Poisson PMF have more reliability as it is not only the
575 unbiasedness and consistency of the MLE of λ , but also the UMVUE of MLE. The
576 UMVUE in Poisson PMF implied that lowest variance unbiased estimator can make
577 the Poisson PMF to be more steadily and accurately stimulate the stochasticity of soil
578 erosion events over long-term observation than binomial PMF.

579 Thirdly, besides having better simulation of the stochastic soil erosion events at larger
580 temporal scale, the Poisson PMF could also be more suitable for simulating the
581 randomness of S event in the closed-design plot system than that of binomial PMF.

582 As the hypothesis of Boix-Fayos et al in 2006, the closed runoff-plot design forms
583 an obstruction to prevent the transportable material from entering the close monitoring
584 system, which, in particular, lead the transport-limited erosion pattern to gradually
585 transform into detachment-limited pattern in the closed-plot over time (Boix-Fayos et
586 al., 2007; Cammerraat, 2002). Consequently, with the extension of monitoring period,
587 this closed runoff-plot design would cause the sediment more and more difficult to
588 migrate out of plot, which also reduce the probability of observed S events under the
589 same precipitation condition. In fact, the effect of closed runoff-plot on stochastic
590 sediment event could also be successfully implied by the algorithm of Poisson PMF.
591 Specifically, in order to satisfying the fact that $\lambda=np$ in Poisson PMF is an unknown

592 constant, the extension of monitoring period could lead to the numbers of times of I
593 events (n) approach infinity, then the probability (p) of R or S events generation have
594 to approach to zero. Above inference coincides with the assumption about the
595 decreasing of sediment generation in closed-plot system, and further proves that
596 Poisson PMF could be more reliable to simulate the stochastic erosion events at longer
597 temporal scale.

598

599 **5.2 The effect of influencing factors on erosion stochasticity**

600 The effects of rainfall, soil and vegetation properties on erosion stochasticity in different
601 restoration vegetation types were evaluated by LRM. It integrated stochastic rainfall
602 events with their precipitation and intensity grades, and connected the ecohydrological
603 functions of soil and plant with their classified hydrological and morphological features.
604 Just as serving as previous studies (Verheyen and Hermy, 2001a, 2001b; Verheyen et
605 al., 2003 and Hermy, 2001a; 2001b; Verheyen et al., 2003), LRM in this study explored
606 the relative importance of morphological features disturbing on the transmission of
607 stochastic signal of I events into R and S events in different restoration vegetation types.
608 These disturbances are closed related to the complex hydrological functions owned by
609 different morphological structures, which finally affect the whole processes of runoff
610 production and sediment yield (Bautista et al., 2007; Puigdefàbregas, 2005).

611 First, many previous field experiments and mechanism models have proved that
612 canopy structure has capacity for intercepting intercept precipitation. This specific
613 hydrological function could potentially prevent the rainfall from directly forming

614 overland flow or splashing soil surface particles (Liu, 2001; Mohammad and Adam,
615 2010; Morgan, 2001; Wang et al., 2012). The precipitation retention owned by canopy
616 structure was regarded as an indispensable positive factor to reduce the soil erosion rate.
617 Meanwhile, as a crucial complement to understanding hydrological function of canopy
618 structure, the result of LRM in this study indicated that the higher-grade canopy
619 structure was a most important morphological feature to reduce the odds ratio of
620 random soil events in all restoration vegetation types. This result suggests that, the
621 larger canopy diameter would have relatively stronger capacity for disturbing the
622 transmission processes of stochastic signal of rainfall on the soil surface than that of
623 other morphological properties. From the perspective of erosion stochasticity, the
624 higher-grade canopy structure could finally attribute to the lower probability of R and
625 S event generation. Therefore, the diversity of canopy structures in different vegetation
626 types could act a key role on both reducing the intensity and probability of soil erosion
627 generation.

628 Secondly, many studies have also discovered that the denser root system distributing
629 in soil matrix could improve the reinfiltration of the overland (Gyssels et al., 2005).
630 This reinfiltration process is an effective way to recharge soil water stores when the
631 overland flow started to occur in hillslopes, which was also an indispensable
632 contributing factor to reduce the unit area runoff production (Moreno-de las Heras et
633 al., 2009; Moreno-de las Heras et al., 2010). In this study, the potential reinfiltration
634 capacity of soil matrix could be positively affected by the saturated hydraulic soil
635 conductivity (SHC) index. Figure 7 further indicated the distribution patterns of root

636 system in three restoration vegetation types. Meanwhile, the result of LRM also implied
637 that the grade of SHC could negatively affect the odds ratio of stochastic erosion event,
638 which improved the understanding of the hydrological function of root distribution of
639 plant from the view of erosion randomness. It may suggest that the denser root system
640 could create more macropores in the subsurface to provide more probability of
641 reinfiltration of overland flow. This disturbance of overland flow by SHC could reduce
642 the probability of erosion event generation.

643 Thirdly, the litter layer was proved to act multiple roles on conserving the rainfall,
644 improving infiltration of throughfall, as well as cushioning the splashing of raindrop
645 (Gyssels et al., 2005; Munoz-Robles et al., 2011; Geißler et al., 2012). Therefore, the
646 thicker litter layer in T2 (figure 7) probably has stronger capacity for conserving and
647 infiltrating throughfall, as well as inhibiting splash erosion than that of other restoration
648 vegetation types (Woods and Balfour, 2010). Although the result of LRM indicated that
649 there was no significant correlation between the litter layer thickness (TLL) and the
650 odds ratio of soil erosion (table 6), the interactive effect of TLL and CRO significantly
651 affect the odds ratio of stochastic erosion events (table 7). The interaction result implied
652 that, under the relative low-grade CRO condition, the higher-grade TLL could have
653 stronger disturbance on the transmission of stochastic signals of rainfall to improve the
654 throughfall absorption to reduce the probability of splash or sheet erosion occurrence.

655 Additionally, table 7 explored more interactive effects of the soil and plant properties
656 on odds ratio of random runoff and sediment event. These explorations suggested that
657 the interactions between soil and vegetation properties formed more complex

658 hydrological functions to affect the stochastic soil erosion event during whole
659 ecohydrological processes in semi-arid environment (Ludwig et al., 2005).

660 Although the hydrological-trait of vegetation acted as core roles on reducing the soil
661 erosion depending on the mechanical properties of their morphological structures (Zhu
662 et al., 2015), the LRM analysis in this study further illuminated that these hydrological-
663 trait morphological structure of vegetation may also play an important role on affecting
664 the stochasticity of soil erosion. Actually, the different stochasticity of soil erosion in
665 three restoration vegetation types reflected the different extents of disturbance of
666 vegetation types on the transmission of stochastic signals of rainfall into soil-plant
667 systems. Therefore, the relative smaller canopy structure, thinner litter layer, and
668 shallower root system in T3 have relatively weaker capacity to disturbing the stochastic
669 signal of rainfall than that of T1 and T2 with obvious hydrological-trait morphological
670 structures (figure 7). The effect of diverse morphological structures on stochasticity of
671 soil erosion was a meaningful complement to studying on the hydrological functions of
672 restoration vegetation types in semi-arid environment.

673

674 Figure 7

675 Table 6

676 Table 7

677

678

679

680 **5.3 The implication of integrated probabilistic assessment**

681 The integrated probabilistic assessment (IPA) could be an important complement to
682 expand on the understanding of hydrological function existing in vegetation types. The
683 hydrological-trait of morphological structures owned by different plants is closely
684 related to the function of vegetation-driven in affecting the intensity of erosion events.
685 The vegetation-driven-spatial-heterogeneity (VDSH) theory (Puigdefàbregas, 2005)
686 could be regarded as a clear concise summary to emphasize the dominant role of
687 vegetation in restructuring soil erosion processes. It reflected the effect of spatial
688 distribution patterns of vegetation on their corresponding hydrological functions on
689 controlling erosion rate in patch, stand, and even regional scales. Therefore, VDSH
690 theory has provided an innovative view to investigating the soil erosion and other
691 ecohydrological phenomena affected by vegetation (Sanchez and Puigdefàbregas,
692 1994;Puigdefàbregas, 1998;Boer and Puigdefàbregas, 2005). In the study, depending
693 on the long-term experimental data and fundamental probability theories, the IPA
694 concentrated on the hydrological function of vegetation-driven in affecting the
695 randomness of erosion events rather than the erosion rate. It could enrich the
696 comprehension of hydrological function of vegetation morphological structure on soil
697 erosion phenomena, and also be effective complement for application of VDSH theory
698 on interpreting the stochastic erosion events.

699 Additionally, in our study, the IPA could also provide a new framework for
700 practitioners to develop restoration strategies which focused on controlling the risk of
701 erosion generation rather than only on reducing erosion rate. The framework contains

702 three stages including construction of stochastic environment, description of random
703 erosion events, and evaluation of probabilistic attribution (figure 8).

704 The first stage in the framework aims to build a unified platform to describe the
705 stochasticity of different hydrological phenomena closely related to the erosion event.
706 This stage generally investigates the stochastic background under which soil erosion
707 generation, which is also an indispensable precondition for quantifying the probability
708 of R and S in stage II. The second stage is designed to construct a phased adjustment of
709 monitoring processes based on the principle of Bayes theory as well as on the parameter
710 analysis of Binomial and Poisson models. In this phased-adjustment monitoring, the
711 Bayes, Binomial and Poisson models were applied on simulating the randomness of
712 erosion events in short-term, mid-term and long-term monitoring stages, respectively.
713 This model-driven monitoring approach could be regarded as a more reasonable method
714 to explore the complexity of stochastic erosion events in larger temporal scales, but also
715 provide a new perspective for researchers to more effectively evaluate the stochasticity
716 of erosion events in stage III. The objective of stage III is to assess the probabilistic
717 attribution of rainfall, soil and vegetation properties on erosion events generation. This
718 probabilistic attribution evaluation by LRM, could develop the restoration strategies for
719 more effectively selecting vegetation types with stronger capacity for reducing the
720 erosion risk, and finally improve the management of soil and water conservation in a
721 semi-arid environment.

722 As a result, this stochasticity-based restoration strategy was developed by a
723 combination of experimental data with multiple probabilistic theories to deal with the

724 soil erosion randomness under complex stochastic environment. It is different from the
725 trait-based restoration scheme derived from the functional diversity of vegetation
726 community to reduce the soil erosion rate (Zhu et al., 2015; Baetas et al., 2009).
727 Meanwhile, with the increase of monitoring duration, more stochastic information of
728 erosion events could be added into the IPA framework. This addition could finally fulfil
729 the self-renewal and self-adjustment of the IPA to improve the restoration strategy for
730 selecting more reasonable vegetation types with stronger capacity for controlling
731 erosion risk in long term. Therefore, the IPA framework containing three stages could
732 translate the event-driven erosion stochasticity into restoration strategies concentrating
733 on erosion randomness, which may be a meaningful complement for restoration
734 management in a semi-arid environment.

735

736  Figure 8

737

738 **6. Conclusion**

739 In this study, we applied an integrated probabilistic assessment (IPA) to describe,
740 simulate and evaluate the stochasticity of soil erosion in three restoration vegetation
741 types in the Loess Plateau of China, and draw the following conclusions:

742 (1) In the IPA, the OCIRS was an innovative event-driven system to standardize the
743 definition of hydrological random events, which is also a foundation for quantifying
744 the stochasticity of soil erosion events under complex environment conditions.

745 (2) Both of binomial and Poisson PMFs in the IPA could simulate the probability

746 distribution of the numbers of runoff and sediment events in all restoration
 747 vegetation types. However, Poisson PFM could more effectively simulate the
 748 stochasticity of soil erosion at larger temporal scales.

749 (3) The difference of morphological structures in restoration vegetation types is the
 750 main source of different stochasticity of soil erosion from T1 to T3 under same
 751 rainfall condition. Larger canopy, thicker litter layer and denser root distribution
 752 could more effectively affect the transmission of stochastic signal of rainfall into
 753 soil erosion.

754 The IPA is an important complement to developing restoration strategies to improve
 755 the understanding of stochasticity of erosion generation rather than only of the intensity
 756 of erosion event. It could also be meaningful to researchers and practitioners to evaluate
 757 the efficacy of soil control practices in a semi-arid environment.

758

759 **Appendix A. The transformation from binominal to Poisson PMF**

760 Let $p = \frac{\lambda}{n}$, then:

$$\begin{aligned}
 761 \quad pmf_{Xbin}(x) &= \binom{n}{x} p^x (1-p)^{n-x} = \frac{n!}{x!(n-x)!} \cdot \left(\frac{\lambda}{n}\right)^x \cdot \left(1 - \frac{\lambda}{n}\right)^{n-x} \\
 762 \quad &= \frac{\lambda!}{x!} \cdot \frac{n(n-1)(n-2)\cdots 1}{(n-x)(n-x-1)\cdots 1} \cdot \frac{1}{n^x} \cdot \left(1 - \frac{\lambda}{n}\right)^{n-x} \\
 763 \quad &= \frac{\lambda!}{x!} \cdot 1 \cdot \left(1 - \frac{1}{n}\right) \cdot \left(1 - \frac{2}{n}\right) \cdots \left(1 - \frac{x-1}{n}\right) \cdot \left(1 + \frac{-\lambda}{n}\right)^n \cdot \left(1 - \frac{\lambda}{n}\right)^{-x} \quad (A1)
 \end{aligned}$$

764 In equation (A1), when $n \rightarrow \infty$, and x, λ is finite and constant, then

$$765 \quad \lim_{n \rightarrow \infty} \left(1 - \frac{1}{n}\right) = \cdots = \lim_{n \rightarrow \infty} \left(1 - \frac{x-1}{n}\right) = \lim_{n \rightarrow \infty} \left(1 - \frac{\lambda}{n}\right)^{-x} = 1 \quad (A2)$$

766 And

$$767 \quad \lim_{n \rightarrow \infty} \left(1 + \frac{-\lambda}{n}\right)^n = e^{-\lambda} \quad (A3)$$

768 And according to equation (A2) and (A3), the equation (A1) can be transformed as:

$$769 \quad \lim_{n \rightarrow \infty} \left[\frac{n!}{x!(n-x)!} \cdot \left(\frac{\lambda}{n}\right)^x \cdot \left(1 - \frac{\lambda}{n}\right)^{n-x} \right] = \frac{\lambda^x e^{-\lambda}}{x!} \quad x = 0, 1, 2, \dots \quad (A4)$$

770 or

$$771 \quad pmf_{Xbin}(x) \xrightarrow{n \rightarrow \infty} \frac{\lambda^x e^{-\lambda}}{x!} = pmf_{Xpoi}(x) \quad (A5)$$

772

773 **Appendix B. Parameter estimation of p in Poisson PMF**

774 **(1) Derivatization of the MLE \hat{p}**

775 Let the random sample $X_1, X_2, \dots, X_i \xrightarrow{iid} pmf_{Xbin}(p)$ and assume the binomial
776 distribution as:

$$777 \quad P(X = x_i) = \binom{m}{x_i} p^{x_i} (1-p)^{m-x_i} \quad (B1)$$

778 The likelihood function $L(p)$ is joint binomial PDF with parameter p as follow:

$$779 \quad L(p) = f_X(X_1, \dots, X_n, p) = \prod_{i=1}^n \binom{m}{x_i} p^{\sum_{i=1}^n x_i} (1-p)^{(mn - \sum_{i=1}^n x_i)} \quad (B2)$$

780 By taking logs on both side of equation (B2):

$$781 \quad \ln L(p) = \ln \left(\prod_{i=1}^n \binom{m}{x_i} \right) + \sum_{i=1}^n x_i \ln p + \left(mn - \sum_{i=1}^n x_i \right) \ln(1-p) \quad (B3)$$

782 And differentiating with respect to p in $\ln L(P)$ and let the result be zero:

$$783 \quad \frac{\partial \ln L(p)}{\partial p} = \frac{\sum_{i=1}^n x_i}{p} - \frac{(mn - \sum_{i=1}^n x_i)}{(1-p)} = 0 \quad (B4)$$

$$784 \quad \text{Solution } \hat{p} = \frac{\sum_{i=1}^n x_i}{mn}, \text{ let } m = n, \Rightarrow \hat{p} = \frac{\bar{X}}{n}$$

785 Therefore, $\hat{p} = \frac{\bar{X}}{n}$ is the MLE of population parameter p in binomial PMF model.

786

787 **(2) Discussion of the unbiasedness and consistency of \hat{p}**

788 Let $E_p(\hat{p})$ be the expectation of M.L.E \hat{p} when population parameter p is true in

789 random sample which is $X_1, X_2, \dots, X_i \xrightarrow{iid} pmf_{Xbin}(p)$, then

$$790 \quad E_p(\hat{p}) = E_p(\bar{X}/n) = \frac{1}{n^2} \sum_{i=1}^n E_p(X_i) = \frac{1}{n^2} n^2 p = p \quad (B5)$$

791 Which proved that MLE $\hat{p} = \frac{\bar{X}}{n}$ is a unbiased estimator for p . And furthermore then

792 let $Var_p(\hat{p})$ be the variance of \hat{p} when population p is true.

$$793 \quad Var_p(\hat{p}) = Var_p\left(\sum_{i=1}^n X_i/n^2\right) = \frac{1}{n^4} \sum_{i=1}^n Var_p(X_i) = \frac{p(1-p)}{n^2} \quad (B6)$$

794 As the n approaches to infinite:

$$795 \quad \lim_{n \rightarrow \infty} Var_p(\hat{p}) = \lim_{n \rightarrow \infty} \left(\frac{p(1-p)}{n^2}\right) = 0 \quad (B7)$$

796 Equation (B5)~(B7) satisfied the theme of weak law of larger number, which lead the

797 $\hat{p} = \frac{\bar{X}}{n}$ is probabilistic converge to population parameter p :

$$798 \quad \lim_{n \rightarrow \infty} P(|\hat{p} - p| \geq \varepsilon) = 0, \text{ for all } \varepsilon > 0 \quad (B8)$$

799 Consequently, the unbiased MLE $\hat{p} = \frac{\bar{X}}{n}$ is consistent for p .

800

801 **Appendix C. Parameter estimation of λ in Poisson PMF**

802 **(1) Derivatization of the MLE $\hat{\lambda}$**

803 Let the random sample $X_1, X_2, \dots, X_i \xrightarrow{iid} pmf_{Xpoi}(\lambda)$, and assume the poisson

804 distribution as:

$$805 \quad pmf_{Xpoi}(x_i) = \frac{\lambda^{x_i} e^{-\lambda}}{x_i!} \quad (C1)$$

806 The likelihood function $L(\lambda)$ is joint PDF with parameter λ as follow:

$$807 \quad L(\lambda) = f_X(X_1, \dots, X_n, \lambda) = f(X_1, \lambda) \times \dots \times f(X_n, \lambda) = \prod_{i=1}^n \frac{\lambda^{x_i} e^{-\lambda}}{x_i!} \quad (C2)$$

808 Taking logs on $L(\lambda)$ in equation (B4) and differentiating logarithm function with

809 respect to λ :

$$810 \quad \frac{\partial \ln L(\lambda)}{\partial \lambda} = \frac{\partial \left(\prod_{i=1}^n \frac{\lambda^{x_i} e^{-\lambda}}{x_i!} \right)}{\partial \lambda} = -n \frac{\lambda^{\sum_{i=1}^n x_i}}{(x_1 x_2 \cdots x_n)!} e^{-n\lambda} + \frac{\sum_{i=1}^n X_i \lambda^{(-1+\sum_{i=1}^n x_i)}}{(x_1 x_2 \cdots x_n)!} \quad (C3)$$

811 Let the equation (C3) equal to zero, and has solution:

$$812 \quad \hat{\lambda} = \frac{1}{n} \sum_{i=1}^n X_i = \bar{X} \quad (C4)$$

813 Therefore, $\hat{\lambda} = \bar{X}$ is the MLE of population parameter λ in Poisson PMF model.

814

815 (2) Discussion of the unbiasedness and consistency of $\hat{\lambda}$

816 Let $E_{\lambda}(\hat{\lambda})$ be the expectation of MLE $\hat{\lambda}$ when population parameter λ is true in

817 random sample $X_1, X_2, \dots, X_i \xrightarrow{iid} pmf_{X_{poi}}(\lambda)$, then:

$$818 \quad E_{\lambda}(\hat{\lambda}) = E_{\lambda}(\bar{X}) = \frac{1}{n^2} \sum_{i=1}^n E_{\lambda}(X_i) = \frac{1}{n} n\lambda = \lambda \quad (C5)$$

819 which proved that MLE $\hat{\lambda} = \bar{X}$ is a unbiased estimator for λ . Meanwhile, let $Var_{\lambda}(\hat{\lambda})$

820 be the variance of MLE $\hat{\lambda}$ when population parameter λ is true

$$821 \quad Var_{\lambda}(\hat{\lambda}) = Var_{\lambda}(\bar{X}) = Var_{\lambda} \left(\sum_{i=1}^n X_i / n^2 \right) = \frac{1}{n^4} \sum_{i=1}^n Var_{\lambda}(X_i) = \frac{\lambda}{n} \quad (C6)$$

822 And

$$823 \quad \lim_{n \rightarrow \infty} Var_{\lambda}(\hat{\lambda}) = \lim_{n \rightarrow \infty} \left(\frac{\lambda}{n} \right) = 0 \quad (C7)$$

824 According to the weak law of large number theme, equation (B7, B8, C1) lead that

825 unbiased MLE $\hat{\lambda} = \bar{X}$ is probabilistic converge to λ :

$$826 \quad \lim_{n \rightarrow \infty} P(|\hat{\lambda} - \lambda| \geq \varepsilon) = 0, \text{ for all } \varepsilon > 0 \quad (C8)$$

827 Therefore, MLE $\hat{\lambda} = \bar{X}$ is consistent for population parameter λ .

828

829 (3) Determination of UMVUE $\hat{\lambda}$ of population parameter

830 Firstly, MLE $\hat{\lambda} = \bar{X}$ is an unbiased estimator of parameter λ which is the

831 precondition of UMVUE determination. Secondly, by using Cramer-Rao lower bound

832 to check whether the unbiased MLE was UMVUE or not. Then we have:

$$833 \quad \ln f_X(X, \lambda) = -\ln x! + x \ln \lambda - \lambda \quad (C9)$$

$$834 \quad \frac{\partial(\ln f_X(X, \lambda))}{\partial \lambda} = \frac{x}{\lambda} - 1 \quad (C10)$$

835 And

$$836 \quad \frac{\partial^2 \ln f_X(X, \lambda)}{\partial \lambda^2} = \frac{\partial(\frac{x}{\lambda} - 1)}{\partial \lambda} = -\frac{x}{\lambda^2} \quad (C11)$$

837 Accordingly the expectation of equation (C11) when the population parameter λ is
838 true:

$$839 \quad E_\lambda \left[\frac{\partial^2 \ln f_X(X, \lambda)}{\partial \lambda^2} \right] = E_\lambda \left(-\frac{X}{\lambda^2} \right) = -\frac{1}{\lambda^2} E_\lambda(X) = -\frac{\lambda}{\lambda^2} = -\frac{1}{\lambda} \quad (C12)$$

840 So the Cramer-Rao lower bound (CRLB) is

$$841 \quad \text{CRLB} = \frac{1}{-n E_\lambda \left[\frac{\partial^2 \ln f_X(X, \lambda)}{\partial \lambda^2} \right]} = \frac{1}{-n \cdot (-\frac{1}{\lambda})} = \frac{\lambda}{n} = \text{Var}_\lambda(\hat{\lambda}) = \text{Var}_\lambda(\bar{X}) \quad (C13)$$

842 Consequently, MLE $\hat{\lambda} = \bar{X}$ is UMVUE of population parameter λ .

843

844 **Acknowledgement**

845 This work was funded by the National Natural Science Foundation of China (No.
846 41390464) and the National Key Research and Development Program (No.
847 2016YFC0501602). We specially thank for associated editor, and two reviewers whose
848 suggestions and advices improve the quality of this study, we also thank professor Chen
849 Lin-An with National Chiao Tung University (NCTU) for his great help on the
850 mathematical statistical inference in this manuscript, and thank Liu Yu, Liu Jianbo and
851 Wang Jian for their support for soil erosion monitoring.

852

853 **Figure captions**

854 Figure 1 The construction of OCIRS system : (a) a flow chart to determine all random event types
855 in OCIRS framework; (b) the different combining patterns of rainfall and non-rainfall events in three
856 consecutive days to form ten observed random event sequences on five rainy seasons; (c) Venn
857 diagram to reveal the relationship among all random events types in OCIRS framework.

858

859 Figure 2 Study area and experimental design: (a) location of the Yangjuangou Catchment; (b)
860 three restoration vegetation types including *Armeniaca sibirica* (T1), *Spiraea pubescens* (T2), and
861 *Artemisia copria* (T3); (c) the dynamic measurement of soil moisture and data collection to provide
862 the information about average antecedent soil moisture; (d) the measurement of field saturated
863 hydraulic conductivity to determine the average infiltration capability; (e): the investigation of
864 morphological properties of restoration vegetation by setting quadrats

865

866 Figure 3 The probability distribution of different random rainfall event types (Iw, Is, Il, and Ie)
867 and random non-rainfall event types (Ch and Cd) at monthly and seasonal scales from rainy season
868 of 2008 to 2012.

869

870 Figure 4 The probability distribution of random runoff and sediment events generating in three
871 restoration vegetation types at monthly and seasonal scales from rainy season of 2008 to 2012, the
872 Arabic numbers and letter “T” on the abscissa indicate the month and season respectively, the same
873 as follow figures

874

875 Figure 5 The comparison between simulation of stochasticity of runoff and sediment events by
876 Binomial and Poisson PMFs and the observed frequencies of numbers of times of soil erosion events
877 in three restoration vegetation type, Exp_B and Exp_P indicates the simulated values in Binomial
878 and Poisson PMF respectively, and the histogram represents the observed values.

879

880 Figure 6 The distribution of probabilistic contribution of four random rainfall event types on
881 anyone runoff or sediment event stochastically generating in three restoration vegetation types at
882 monthly and seasonal scales from rainy season of 2008 to 2012

883

884 Figure 7 Morphological properties of three restoration vegetation types including the thickness
885 of litter layer, the distribution of root system. The dashed lines indicates the diameter and depth of
886 soil samples with approximating 10 cm and 30 cm respectively.

887

888 Figure 8 The framework of integrated probabilistic assessment for soil erosion monitoring and
889 restoration strategies

890

891 **Reference**

- 892 Andres-Domenech, I., Montanari, A., and Marco, J. B.: Stochastic rainfall analysis for storm tank
893 performance evaluation *Hydrology and Earth System Sciences*, 14, 1221-1232, 2010.
- 894 Baetas, S. D., Poesen, J., Reubens, B., Muys, B., Baerdemaeker, D., and Meersmans, J.:
895 Methodological framework to select plant species for controlling rill and gully erosion:
896 application to a Mediterranean ecosystem, *Earth Surface Processes and Landforms*, 34, 1374-
897 1392, 2009.
- 898 Bautista, S., Mayor, A. G., Bourakhouadar, J., and Bellot, J.: Plant spatial pattern predicts hillslope
899 runoff and erosion in a semiarid Mediterranean landscape, *Ecosystems*, 10, 987-998, 2007.
- 900 Bhunya, P. K., Berndtsson, R., Ojha, C. S. P., and Mishra, S. K.: Suitability of Gamma, Chi-square,
901 Weibull, and Beta distributions as synthetic unit hydrographs, *Journal of Hydrology*, 334, 28-38,
902 2007.
- 903 Boer, M., and Puigdefàbregas, J.: Effects of spatially structured vegetation patterns on hillslope
904 erosion in a semiarid Mediterranean environment: a simulation study, *Earth Surface Processes
905 and Landforms*, 30, 149-167, 2005.
- 906 Boix-Fayos, C., Martinez-Mena, M., Arnau-Rosalen, E., Calvo-Cases, A., Castillo, V., and
907 Albaladejo, J.: Measuring soil erosion by field plots: Understanding the sources of variation.,
908 *Earth-Science Reviews*, 78, 267-285, 2006.
- 909 Boix-Fayos, C., Martinez-Mena, M., Calvo-Cases, A., Arnau-Rosalen, E., Albaladejo, J., and
910 Castillo, V.: Causes and underlying processes of measurement variability in field erosion plots in
911 Mediterranean conditions, *Earth Surface Processes and Landforms*, 32, 2007.
- 912 Bonham, C.: *Measurements for Terrestrial Vegetation*, second ed., John Wiley & Sons. Ltd, 1989.
- 913 Cammeraat, L. H.: A review of two strongly contrasting geomorphological systems within the
914 context of scale, *Earth Surface Processes and Landforms*, 27, 1201-1222, 2002.
- 915 Cantón, Y., Solé-Benet, A., de Vente, J., Boix-Fayos, C., Calvo-Cases, A., Asensio, C., and
916 Puigdefàbregas, J.: A review of runoff generation and soil erosion across scales in semiarid south-
917 eastern Spain, *Journal of Arid Environments*, 75, 1254-1261, 2011.
- 918 Cao, S. X., Chen, L., and Yu, X. X.: Impact of China's Grain for Green Project on the landscape of
919 vulnerable arid and semi-arid agricultural regions: a case study in northern Shaanxi Province,
920 *Journal of Applied Ecology*, 46, 536-543, 2009.
- 921 Castillo, V., Gomezplaza, A., and Martinezmena, M.: The role of antecedent soil water content in
922 the runoff response of semiarid catchments: a simulation approach, *Journal of Hydrology*, 284,
923 114-130, 2003.
- 924 Eagleson, P. S.: Climate, soil and vegetation 2. The distribution of annual precipitation derived from
925 observed storm sequences, *Water Resource Research*, 14, 713-721, 1978.
- 926 FAO-UNESCO: *Soil map of the world (1:5000000)*, Food and agriculture organization of the Unite
927 Nations, UNESCO, Paris, 1974.
- 928 Freeze, R. A.: A Stochastic-Conceptual Analysis of Rainfall-Runoff Processes on a Hillslope, *Water
929 Resource Research*, 16, 391-408, 1980.
- 930 Fu, B., Liu, Y., He, C., Zeng, Y., and Wu, B.: Assessing the soil erosion control service of ecosystems
931 change in the Loess Plateau of China, *Ecology Complexity*, 8, 284-293, 2011.
- 932 Geißler, C., Kühn, P., Böhnke, M., Bruehlheide, H., Shi, X., and Scholten, T.: Splash erosion potential
933 under tree canopies in subtropical SE China, *Catena*, 91, 85-93, 2012.

934 Gyssels, G., Poesen, J., Bochet, E., and Li, Y.: Impact of plant roots on the resistance of soils to
935 erosion by water: a review, *Progress in Physical Geography*, 29, 189-217, 2005.

936 Haberlandt, U., and Radtke, I.: Hydrological model calibration for derived flood frequency analysis
937 using stochastic rainfall and probability distributions of peak flows, *Hydrology and Earth System
938 Sciences*, 18, 353-365, 2014.

939 Hosmer, W., Lemeshow, S., and Sturdivant, R.: *Applied Logistic Regression*, Third ed., John Willey
940 & Sons. Inc., 2013.

941 Janzen, D., and McDonnell, J. J.: A stochastic approach to modelling and understanding hillslope
942 runoff connectivity dynamics, *Ecological Modelling*, 298, 64-74, 2015.

943 Jiang, Z., Su, S., Jing, C., Lin, S., Fei, X., and Wu, J.: Spatiotemporal dynamics of soil erosion risk
944 for Anji County, China, *Stochastic Environmental Research and Risk Assessment*, 26, 751-763,
945 2012.

946 Jiao, J., Wang, W., and Hao, X.: Precipitation and erosion characteristics of rain-storm in different
947 pattern on Loess Plateau, *Journal of Arid Land Resources and Environment*, 13, 34-42, 1999.

948 Kim, J., Ivanov, V., and Fatichi, S.: Environmental stochasticity controls soil erosion variability
949 *Scientific Report*, 6, 10.1038/srep22065, 2016.

950 Liu, S.: Evaluation of the Liu model for predicting rainfall interception in forest world-wide,
951 *Hydrological Processes*, 15, 2341-2360, 2001.

952 Liu, Y., Fu, B., Lü, Y., Wang, Z., and Gao, G.: Hydrological responses and soil erosion potential of
953 abandoned cropland in the Loess Plateau, China, *Geomorphology*, 138, 404-414, 2012.

954 Lopes, V. L.: On the effect of uncertainty in spatial distribution of rainfall on catchment modelling
955 *Catena*, 28, 107-119, 1996.

956 Ludwig, J. A., Wilcox, B. P., Breshears, D. D., Tongeay, D. J., and Imeson, A. C.: Vegetation patches
957 and runoff-erosion as interacting ecohydrological processes in semiarid landscape, *Ecology* 86,
958 288-297, 2005.

959 Mallick, J., Alashker, Y., Mohammad, S. A.-D., Ahmed, M., and Abul Hasan, M.: Risk assessment
960 of soil erosion in semi-arid mountainous watershed in Saudi Arabia by RUSLE model coupled
961 with remote sensing and GIS, *Geocarto International*, 29, 915-940, 2014.

962 Marques, M. J., Bienes, R., Perez-Rodriguez, R., and Jiménez, L.: Soil degradation in central Spain
963 due to sheet water erosion by low-intensity rainfall events, *Earth Surface Processes and
964 Landforms*, 33, 414-423, 2008.

965 Miao, C. Y., Ni, J., and Borthwick, A. G.: Recent changes in water discharge and sediment load of
966 the Yellow River basin, China, *Progress in Physical Geography*, 34, 541-561, 2010.

967 Mohammad, A. G., and Adam, M. A.: The impact of vegetative cover type on runoff and soil erosion
968 under different land uses, *Catena*, 81, 97-103, 2010.

969 Moore, R. J.: The PDM rainfall-runoff model, *Hydrology and Earth System Sciences*, 11, 483-499,
970 2007.

971 Moreno-de las Heras, M., Merino-Martin, L., and Nicolau, J. M.: Effect of vegetation cover on the
972 hydrology of reclaimed mining soils under Mediterranean-continental climate, *Catena*, 77, 39-47,
973 2009.

974 Moreno-de las Heras, M., Nicolau, J. M., Merino-Martin, L., and Wilcox, B. P.: Plot-scale effects
975 on runoff and erosion along a slope degradation gradient, *Water Resource Research*, 46,
976 10.1029/2009WR007875, 2010.

977 Morgan, R. P. C.: A simple approach to soil loss prediction: a revised Morgan-Finney model, *Catena*,

978 44, 305-322, 2001.

979 Munoz-Robles, C., Reid, N., Tighe, M., Biriggs, S. V., and Wilson, B.: Soil hydrological and
980 erosional responses in patches and inter-patches in vegetation states in semi-arid Australia,
981 *Geoderma*, 160, 524-534, 2011.

982 Portenga, E. W., and Bierman, P. R.: Understanding earth's eroding surface with ¹⁰Be, *GSA Today*,
983 21, 4-10, 2011.

984 Prasannakumar, V., Shiny, R., Geetha, N., and Vijith, H.: Spatial prediction of soil erosion risk by
985 remote sensing, GIS and RUSLE approach: a case study of Siruvani river watershed in Attapady
986 valley, Kerala, India, *Environmental Earth Sciences*, 64, 965-972, 2011.

987 Prooijen, B. C., and Winterwerp, J. C.: A stochastic formulation for erosion of cohesive sediments,
988 *Journal of Geophysical Research* 115, 10.1029/2008JC005189, 2010.

989 Puigdefàbregas, J.: The role of vegetation patterns in structuring runoff and sediment fluxes in
990 drylands, *Earth Surface Processes and Landforms*, 30, 133-147, 2005.

991 Puigdefàbregas, J.: Ecological impacts of global change on drylands and their implications for
992 desertification, *Land Degradation and development*, 9, 393-406, 1998.

993 Puigdefàbregas, J., Solé Benet, A., Gutierrez, L., Barrio, G., and Boer, M.: Scales and processes of
994 water and sediment redistribution in drylands: results from the Rambla Honda field site in
995 Southeast Spain, *Earth Science Reviews*, 48, 39-70, 1999.

996 Ridolfi, L., D'Odorico, P., Porporato, A., and Rodríguez-Iturbe, I.: Stochastic soil moisture dynamics
997 along a hillslope, *Journal of Hydrology*, 272, 264-275, 2003.

998 Robert, V. H., Joseph, W. M., and Allen, T. C.: *Introduction to Mathematical Statistics*, Pearson
999 Education, Inc., 2013.

1000 Rodríguez-Iturbe, I., Porporato, A., Laio, F., and Ridolfi, L.: Plants in water-controlled
1001 ecosystems: active role in hydrologic processes and response to water stress I. Scope and general
1002 outline, *Advances in Water Resources*, 24, 695-705, 2001.

1003 Rodríguez-Iturbe, I., Porporato, A., Ridolfi, L., Isham, V., and Cox, D. R.: Probabilistic modeling of
1004 water balance at a point: the role of climate, soil and vegetation, *Proc R Soc London-Serise A*,
1005 455 3789-3805, 1999.

1006 Sanchez, G., and Puigdefàbregas, J.: Interactions of plant growth and sediment movement on slopes
1007 in a semi-arid environment, *Geomorphology*, 9, 243-360, 1994.

1008 Sheldon, R.: *A first course in probability*, Ninth ed., Pearson Education Limited, 2014.

1009 Sidorchuk, A.: Stochastic modelling of erosion and deposition in cohesive soil *Hydrological*
1010 *Processes*, 19, 1399-1417, 2005.

1011 Sidorchuk, A.: A third generation erosion model: the combination of probabilistic and deterministic
1012 components, *Geomorphology*, 2009, 2-10, 2009.

1013 Verheyen, K., and Hermy, M.: The relative importance of dispersal limitation of vascular plants in
1014 secondary forest succession in Muizen Forest, Belgium, *Journal of Ecology*, 89, 829-840, 2001a.

1015 Verheyen, K., and Hermy, M.: An integrated analysis of the spatio-temporal colonization patterns
1016 of forest plant species in a mixed deciduous forest, *Journal of Vegetation Science*, 12, 567-578,
1017 2001b.

1018 Verheyen, K., Guntenspergen, G., Biesbrouck, B., and Hermy, M.: An integrated analysis of the
1019 effects of past land use on forest herb colonization at the landscape scale, *Journal of Ecology*, 91,
1020 731-742, 2003.

1021 Wang, Fu, B., Piao, S., Lu, Y., Ciais, P., Ciais, P., and Wang, Y.: Reduced sediment transport in the

1022 Yellow River due to anthropogenic changes, *Nature geoscience*, 9, 38-41, 2015.

1023 Wang, G., Gertner, G., Liu, X., and Anderson, A.: Uncertainty assessment of soil erodibility factor
1024 for revised universal soil loss equation, *Catena*, 46, 1-14, 2001.

1025 Wang, G., Gertner, G., Singh, V., Shinkareva, S., Parysow, P., and Anderson, A.: Spatial and
1026 temporal prediction and uncertainty of soil loss using the revised universal soil loss equation: a
1027 case study of the rainfall–runoff erosivity R factor, *Ecological Modelling*, 153, 143-155, 2002.

1028 Wang, P., and Tartakovsky, D. M.: Reduced complexity models for probabilistic forecasting of
1029 infiltration rates, *Advance in Water Resources*, 34, 375-382, 2011.

1030 Wang, S., Fu, B. J., Gao, G. Y., Liu, Y., and Zhou, J.: Responses of soil moisture in different land
1031 cover types to rainfall events in a re-vegetation catchment area of the Loess Plateau, China,
1032 *Catena*, 101, 122-128, 2013.

1033 Wang, X., Zhang, Y., Hu, R., Pan, Y., and Berndtsson, R.: Canopy storage capacity of xerophytic
1034 shrubs in Northwestern China, *Journal of Hydrology*, 454, 152-159, 2012.

1035 Wei, L., and Zhang, W.: *Bayes Analysis*, Press of University of Science and Technology of China,
1036 2013.

1037 Wei, W., L., C., Fu, B., Huang, Z., Wu, D., and Gui, L.: The effect of land uses and rainfall regimes
1038 on runoff and soil erosion in the semi-arid loess hilly area, China, *Journal of Hydrology*, 335,
1039 247-258, 2007.

1040 Wischmeier, W. H., and Smith, D. D.: *Predicting rainfall erosion losses: A guide to conservation
1041 planning*, Agriculture handbook Number 537, United States Department of Agriculture, 1978.

1042 Woods, S. W., and Balfour, V. N.: The effects of soil texture and ash thickness on the post-fire
1043 hydrological response from ash-covered soils, *Journal of Hydrology*, 393, 274-286, 2010.

1044 Yazdi, J., Salehi Neyshabouri, S. A. A., and Golian, S.: A stochastic framework to assess the
1045 performance of flood warning systems based on rainfall-runoff modeling, *Hydrological Processes*,
1046 28, 4718-4731, 2014.

1047 Zhou, J., Fu, B., Gao, G., Lü N., Lü Y., and Wang, S.: Temporal stability of surface soil moisture
1048 of different vegetation types in the Loess Plateau of China, *Catena*, 128, 1-15, 2015.

1049 Zhou, J., Fu, B., Gao, G., Lü Y., Liu, Y., Lü N., and Wang, S.: Effects of precipitation and
1050 restoration vegetation on soil erosion in a semi-arid environment in the Loess Plateau, China,
1051 *Catena*, 137, 1-11, 2016.

1052 Zhu, H., Fu, B., Wang, S., Zhu, L., Zhang, L., and Jiao, L.: Reducing soil erosion by improving
1053 community functional diversity in semi-arid grassland, *Journal of Applied Ecology*,
1054 10.1111/1365-2664.12442, 2015.

1055

1056

1057

1058

1059

1060

1061

1062

1063

1064

1065
1066
1067

Tables

Table 1 The summary of main researches on the stochasticity of soil erosion rate and the stochasticity of factors to affect the soil erosion rate

^a Stochasticity (Uncertainty)	^b Approach or method	^c Driven types	Main Hydrological behaviors	Main Influencing factors	Spatiotemporal Scale	Reference
Stochasticity of soil erosion rate						
Runoff connectivity	Probabilistic model Conceptual model	(1)Data-Mapping (2)Theory	Infiltration processes Precipitation	Topography Soil depth	Hillslope scale in USA	Janzen, D., and McDonnell, J 2015
Runoff processes	Probabilistic model Conceptual model	(1)Simulation (2)Theory	Infiltration processes Precipitation	Topography		Janzen, D., and McDonnell, J 2015
Runoff production	Probabilistic model Conceptual model	(1)Theory (2)Simulation	Runoff absorption Water storage Infiltration capacity	Soil moisture Evaporation Recharge	Point and basin scale	Moore, 2007
Flood prediction and runoff	Probabilistic model Multivariate analysis	(1)Simulation (2)Data-Calibration	Stochastic rainfall process	Parameters in rainfall- runoff model	Multiple catchment scales in Iran	Yazdi, J. et al., 2014
Rainfall and runoff processes	Probabilistic model hydrological mechanism	(1)Simulation (2)Random event (3)Theory	Soil storage	Given climate regime hydraulic conductivity landform development	Hillslope scale	Freeze, 1980
Erosion rate	Probabilistic model Mechanical mechanism	(1)Data-Calculation (2)stochastic forcing		Bed shear stress Critical shear stress	Laboratory scales in Netherlands	Prooijen and Winterwerp, 2010
Erosion rate	Physical model Probabilistic model Conceptual model	(1)Theory (2)Simulation	Simulated near-bed flow	Soil structure Oscillating flow		Sidorchuk, 2005

Erosion risk	Empirical model Geo-statistics	(1)Data-Mapping	Erosive precipitation	Factors in RUSLE	Annual and Regional scales in China	Jiang et al., 2012
Uncertainty of soil loss	Empirical model Geo-statistics Error analysis	(1)Simulation (2)Data-calibration	Erosive precipitation Runoff and sediment	Spatiotemporal Rainfall erosivity distribution	Annual time and catchment scale in USA	Wang et al., 2002
Uncertainty and variability of erosion rate	Empirical model	(1)Hypotheses (2)Data-calculation	Total rainfall volume and 30-minute rainfall intensity	Stochastic environment conditions Scale effect		Kim et al., 2016
Stochasticity of factors to affect soil erosion rate						
Soil moisture related to soil erosion	Probabilistic model Physical model	(1)Hypotheses, (2)Simulation (3)Theory	Precipitation Evapotranspiration	Temporal patterns of rainfall property	Daily time and Hillslope scale in	Ridolfi et al., 2003
Antecedent soil moisture related to soil erosion	Probabilistic model Physical model	(1)Data-Mapping (2)Theory	Runoff response Infiltration processes		Daily time and multiple catchment scales in Spain	Castillo et al., 2003
Stochastic rainfall related to flood and runoff	Probabilistic model Conceptual model	(1)Data-Calibration (2)Random event (3)Hypothesis	Stochastic storm Runoff and flood	Parameters in Peak flow models	Hourly-daily time and multiple catchment scales in Germany	Haberlandt and Radtke, 2014
Stochastic rainfall related to runoff and erosion	Physical model Empirical model	(1)Simulation (2)Data-calibration	Overland/channel flow Erosion transport Precipitation	Spatiotemporal rainfall distribution	Seasonal and annual time catchment scale in USA	Lopes, 1996
Uncertainty of soil erodibility	Empirical model Geo-statistics	(1)Simulation (2)Data-Mapping		Spatiotemporal soil types, depth and parent material	Regional scales in USA	Wang et al., 2001
Stochastic rainfall	Probabilistic model	(1)Data-calibration	Sewer overflows	Rainfall depth and	Seasonal and annual	Andres-

related to runoff	Conceptual model Physical model	(2)Theory	duration, conditions	climate time scales in Spain	catchment Domenech et al., 2010
-------------------	------------------------------------	-----------	-------------------------	------------------------------------	------------------------------------

a: the main contents of different studies focusing on the stochasticity (uncertainty) of soil erosion and its influencing factors

b: the main statistical methods or different types of mathematic and physical models to be employed to describe and analyze the stochasticity of soil erosion

c: the main properties of analyzing framework in the different studies and the characteristics of data application on the evaluation of stochasticity of soil erosion

1068

1069

1070

1071

1072

Table 2 Definition and explanation of all random events in OCIRS

1073

symbol	Physical meaning of random event types	Probabilistic meaning of random event types	Influencing factors and implication
O	observation events with time step ranging from 0 to 72 hours, including non-rainfall and rainfall events	random events composing the sample space of OCIRS system. The probability $P(O) = 1$	indicating the general stochastic weather conditions over rainy seasons
C	non-rainfall events with time step ranging from 0 to 24 hours, including sunny or cloudy weather condition at hour or day scales	random events, the probability of C events is the ratio of numbers of C events to O events $C \subseteq O, 0 \leq P(C) \leq P(O) = 1$	implying the extent of evaporation or potential evapotranspiration in weather condition.
Cd	non-rainfall events with time step being 24 hours, including observed sunny or cloudy at day scale	random events composing the subset of C events, $Cd \subseteq C, 0 \leq P(Cd) \leq P(C)$	implying the duration of evaporation or evapotranspiration at day scale
Ch	non-rainfall events with time step being less than 24hours, including observed sunny or cloudy at hour scales which intercepted by rainfall events within a day	random events composing the subset of C events, the intersection of Ch and Cd is null, $Ch \subseteq C, Cd \cup Ch = C, Cd \cap Ch = \emptyset, 0 \leq P(Ch) \leq P(C)$	influenced by the frequency of rainfall events generation, and implying the alternation of sunny and rainy in a day
I	an individual rainfall event with different precipitation, intensity and duration ranging from 0 to 72 hours, the time interval between two I events is more than 6 hours	random events, the probability of I event is ratio of numbers of I events to O events over observation $I \subseteq O, I \cup C = O, I \cap C = \emptyset, 0 \leq P(I) \leq P(O) = 1$	a driven force of soil erosion, which could be intercepted by vegetation and transformed into throughfall

Ie	an extreme longest individual rainfall event whose average precipitation, intensity and duration were 96.6 mm, 0.022 mm/min, and 73 hours, respectively.	random events composing the subset of I events, $I_e \subseteq I, 0 \leq P(I_e) \leq P(I)$	rainfall events with low intensity and longest duration, inclining to infiltration-excess runoff generation
II	a second longest individual rainfall events types whose average precipitation, intensity and duration were 47.3 mm, 0.027 mm/min, and 30 hours, respectively.	random events composing the subset of I events, the intersection of II and Ie is null, $II \subseteq I, II \cap I_e = \emptyset, 0 \leq P(II) \leq P(I)$	rainfall events with low intensity and long duration, inclining to infiltration-excess runoff generation
Is	A rainfall event type spanning two days whose average precipitation, intensity and duration were 22.7 mm, 0.042 mm/min, and 10 hours, respectively	random events composing the subset of I events, $I_s \subseteq I, I_s \cap II \cap I_e = \emptyset, 0 \leq P(I_s) \leq P(I)$	rainfall events with strongest rainfall intensity in middle duration, inclining to runoff and sediment generation
Iw	a rainfall event type generating within a day whose average precipitation, intensity and duration were 9.8 mm, 0.045 mm/min, and 5 hours, respectively. it usually generates several times within one day.	random events composing the subset of I events, $I_w \subseteq I, I_w \cap I_s \cap II \cap I_e = \emptyset, I_w \cup I_s \cup II \cup I_e = I, 0 \leq P(I_w) \leq P(I)$	rainfall events with fewest and shortest precipitation and duration, which is different to trigger soil erosion
R	runoff event type generating on vegetation land types, it occurs on rainfall processes, and its duration is negligible	random events responding to I events, $R \subset I, R \cap C = \emptyset, 0 \leq P(R) < P(I)$	influenced by rainfall and vegetation properties.
S	sediment event occurring on vegetation land types, it occurs on runoff processes, and its duration is negligible	random events responding to R events, $S \subset R \subset I, S \cap C = \emptyset, 0 \leq P(S) \leq P(R) < P(I)$	driven by R events, and affected by rainfall and vegetation properties.

1074
1075
1076
1077
1078
1079
1080

Table 3 Main characteristics of four types of random rainfall event over five rainy seasons

Rainy season	Rainfall event types	Average precipitation (mm)	Average intensity (mm/min)	Average duration (hour)
2008	Iw	16.7	0.122	2.3
	Is	19.2	0.066	4.8
	II	53.2	0.032	27.7
	Ie	96.6	0.022	73.2
2009	Iw	9.0	0.027	5.6
	Is	35.4	0.059	10.0
	II	47.9	0.032	24.9
	Ie	×	×	×
2010	Iw	9.0	0.018	8.3
	Is	7.6	0.012	10.6
	II	×	×	×
	Ie	×	×	×
2011	Iw	3.3	0.031	1.8
	Is	21.5	0.040	9.0
	II	42.5	0.020	35.4
	Ie	×	×	×
2012	Iw	10.8	0.028	6.4
	Is	30.0	0.031	16.1
	II	45.5	0.023	33.0
	Ie	×	×	×
Average	Iw	9.8	0.045	4.9
	Is	22.7	0.042	10.1
	II	47.3	0.027	30.3
	Ie	96.6	0.022	73.2

1081
1082
1083
1084
1085
1086
1087
1088
1089
1090
1091
1092
1093
1094
1095
1096

1097
1098

Table 4 Basic properties of soil, vegetation and erosion in different restoration vegetation types

Basic properties of different vegetation types	^h N	Restoration vegetation types		
		<i>Armeniaca sibirica</i> Type 1 (T1)	<i>Spiraea pubescens</i> Type 2 (T2)	<i>Artemisia copria</i> Type3 (T3)
Topography property				
Slope aspect	9	Southwest	Southwest	Southwest
Slope gradation (%)	9	≈26.8	≈26.8	≈26.8
Slope size for each (m)	9	3×10	3×10	3×10
Soil property				
^a DBD (g cm ⁻³)	30	1.28±0.08	1.16±0.12	1.23±0.10
Clay (%)	30	11.07±2.43	11.98±3.05	9.54±1.48
Silt (%)	30	26.11±1.50	25.24±3.84	26.72±2.87
Sand (%)	30	62.82±0.94	62.78±4.51	63.74±3.24
^b Texture type		Sandy loam	Sandy loam	Sandy loam
^c SHC (cm min ⁻¹)	20	0.46±0.82(a)	2.22±0.66(b)	0.50±0.60(a)
^d SOM (%)	30	1.28±0.63(a)	0.98±0.15(b)	0.90±0.09(b)
Vegetation property				
Restoration years	9	20	20	20
Crown diameters (cm)	27	211.6±15.4(c)	80.5±4.5(b)	64.1±6.3(a)
Litter layer (cm)	30	1.2±0.3(a)	3.4±1.8(b)	1.8±0.5(a)
Height (cm)	27	256.3±11.1(c)	128.3±8.3(b)	61.8±1.1(a)
LAI	27	×	2.31	1.78
^e Ave. Coverage (%)	27	85	90	90
Rainfall/Erosion property				
Times of rainfall events			130	
Times of runoff events		30/30/30	45/45/45	45/45/45
Times of sediment events		13/13/13	19/19/19	32/32/32
^f Ave. runoff depth (cm)		0.012(a)	0.014(a)	0.083(b)
^g Ave. sediment amount (g)		5.8(a)	6.8(a)	25.7(b)

a: dry bulk density; b: texture type is determined by textural triangle method based on USDA; c: field saturated hydraulic conductivity, and all the values with same letter in each row indicates non-significant difference at $\alpha=0.05$ which is the same as follow rows; d: soil organic matter; e: average coverage of three restoration vegetation types over five rainy seasons; f: average runoff depth in restoration types over rainy seasons; g: average sediment yield in restoration types over rainy seasons; h: sample number.

1099
1100
1101
1102
1103
1104
1105

1106 Table 5 The definition and classification of properties of rainfall soil and plant ordinal variables
 1107

Ordinal variable	Physical meaning of classified influencing factors	Standard of influencing factor classification			
		Low (L)	Middle (M)	High (H)	Extreme (E)
PREC	classified precipitation variable of a single random rainfall event	0~15 mm	15~30 mm	30~60 mm	>60 mm
INT	classified intensity variable of a single random rainfall event	0~0.025 mm/min	0.025~0.05 mm/min	0.05~0.1 mm/min	>0.1 mm/min
ASM	classified variable of the antecedent soil moisture	0~5 %	5~10 %	10~20 %	>20 %
SHC	classified variable of the filed saturated hydraulic conductivity	0~1 cm/min	×	>1 cm/min	×
CRO	classified variable of the average crown width in vegetation types	0~60 cm	60~80 cm	>80 cm	×
TLL	classified variable of the average thickness of litter layers	0~2 cm	×	>2 cm	×
Y_R	dichotomous dependent variable to indicate whether a random runoff event has generation or not	If $Y_R = 1$, it means that a random runoff event has generated; If $Y_R = 0$, it means that a random runoff event has not generated			
Y_S	dichotomous dependent variable to indicate whether a random sediment event has generation or not	If $Y_S = 1$, it means that a random sediment event has generated; If $Y_S = 0$, it means that a random sediment event has not generated			

1108
 1109
 1110
 1111
 1112
 1113
 1114
 1115
 1116
 1117
 1118
 1119
 1120
 1121
 1122
 1123
 1124
 1125
 1126
 1127
 1128

1129 Table 6 Logistic regression model to analysis the single effect of rainfall, plant and soil ordinal
 1130 variable on the erosion events presence/absence in all restoration vegetation types
 1131

Grade levels	PREC (Low)	INT (Low)	ASM (Low)	SHC (Low)	CRO (Low)	TLL (Low)
Odds ratio of all random runoff events						
Extreme	^a × ^{NS}	^b 90.91***	^c 2.19*	Null	Null	Null
High	× ^{NS}	32.26***	2.01*	^d 0.85*	^e 7.53×10 ⁻³ **	^f × ^{NS}
Middle	× ^{NS}	2.09*	1.59*	Null	7.17×10 ⁻² **	Null
Odds ratio of all random sediment events						
Extreme	142.85***	166.67***	15.40*	Null	Null	Null
High	16.95**	125.00***	13.79**	0.78*	6.27×10 ⁻³ **	× ^{NS}
Middle	6.09**	34.48***	6.36*	Null	2.55×10 ⁻² **	Null

a: making the low-grade of PREC ordinal variable as reference, the odds ratio of all random runoff event in extreme-grade of PREC is not significantly larger than that of low-grade of PREC; b: making the low-grade of INT ordinal variable as reference, the odds ratio of all random runoff events in extreme-grade of INT is 90.91 times significantly larger than that of low-grade of INT, under the controlled PREC condition with P≤0.001; c: making the low-grade of ASM ordinal variable as reference, the odds ratio of all random runoff events in extreme-grade of ASM is 2.19 times significantly larger than that of low-grade of ASM, under the controlled PREC and INT condition with P≤0.1; d: making the low-grade of SHC ordinal variable as reference, the odds ratio of all random runoff events in high-grade of SHC is 0.85 times significantly larger than that of low-grade of SHC, under the controlled PREC, INT and ASM condition with P≤0.1; e: making the low-grade of CRO ordinal variable as reference, the odds ratio of all random runoff events in high-grade of CRO is 7.53×10⁻³ larger than that of low-grade of CRO, under the controlled PREC, INT, ASM and SHC condition with P≤0.01; f: making the low-grade of TLL ordinal variable as reference, the odds ratio of all random runoff event in high-grade of TLL is not significantly larger than that of low-grade of TLL, under the controlled PREC, INT, ASM, SHC and CRO condition. (Wald test statistic is applied to test the significant of odds ratio *** P≤0.001, ** P≤0.01, * P≤0.1, NS: not significant, ×^{NS}: the nonsignificant value cannot be estimated)

1132
 1133
 1134
 1135
 1136
 1137
 1138
 1139
 1140
 1141
 1142
 1143
 1144
 1145

1146 Table 7 Logistic regression model to analysis the interactive effect of rainfall, plant and soil
 1147 ordinal variables on the erosion events presence/absence in all restoration vegetation types
 1148

Grade levels	Reference of grade levels	Soil_ASM				Plant_TLL	
		ASM (low)	ASM (middle)	ASM (high)	ASM (extreme)	TLL (low)	TLL (high)
Odds ratio of all random runoff events							
Soil_SHC	SHC (low)	Ref.	^a 2.23 ^{NS}	3.19 ^{NS}	7.02*	Null	Null
Plant_TLL	TLL (Low)	Ref.	2.23 ^{NS}	3.19 ^{NS}	7.02*	Null	Null
Plant_CRO	CRO (low)	Ref.	^b 64.34*	70.77*	486.43**	Ref.	^c 0.12***
	CRO(middle)	Ref.	× ^{NS}	2.32 ^{NS}	22.49*	Null	Null
	CRO (high)	Ref	Null	Null	Null	Null	Null
Odds ratio of all sediment runoff events							
Soil_SHC	SHC (low)	Ref.	× ^{NS}	1.22 ^{NS}	1.82 ^{NS}	Null	Null
Plant_TLL	TLL (Low)	Ref.	× ^{NS}	1.22 ^{NS}	1.82 ^{NS}	Null	Null
Plant_CRO	CRO (low)	Ref.	× ^{NS}	× ^{NS}	× ^{NS}	Ref.	0.33**
	CRO(middle)	Ref.	× ^{NS}	× ^{NS}	× ^{NS}	Null	Null
	CRO (high)	Ref	Null	Null	Null	Null	Null

a: making the interactive effect of low-grade of SHC and low-grade of ASM as reference, the odds ratio of all random runoff events affected by the interactive effect of low-grade of SHC and middle-grade of ASM is 2.23 times larger than that interactive effect of low-grade SHC and low-grade of ASM under controlled rainfall conditions; b: making the interactive effect of low-grade of CRO and low-grade of ASM as reference, the odds ratio of all random runoff events affected by the interactive effect of low-grade of CRO and middle-grade of ASM is 64.34 times significantly larger than that interactive effect of low-grade of CRO and low-grade of ASM under controlled rainfall conditions, with $P \leq 0.1$; c: making the interactive effect of low-grade of CRO and low-grade of TLL as reference, the odds ratio of all random runoff events affected by the interactive effect of low-grade of CRO and high-grade of TLL is 0.12 times significantly larger than that interactive effect of low-grade of CRO and low-grade of TLL, with $P \leq 0.001$ (Wald test statistic is applied to test the significant of odds ratio *** $P \leq 0.001$, ** $P \leq 0.01$, * $P \leq 0.1$, NS: not significant, ×^{NS}: the nonsignificant value cannot be estimated)

1149
 1150
 1151
 1152
 1153
 1154
 1155
 1156
 1157
 1158
 1159
 1160
 1161

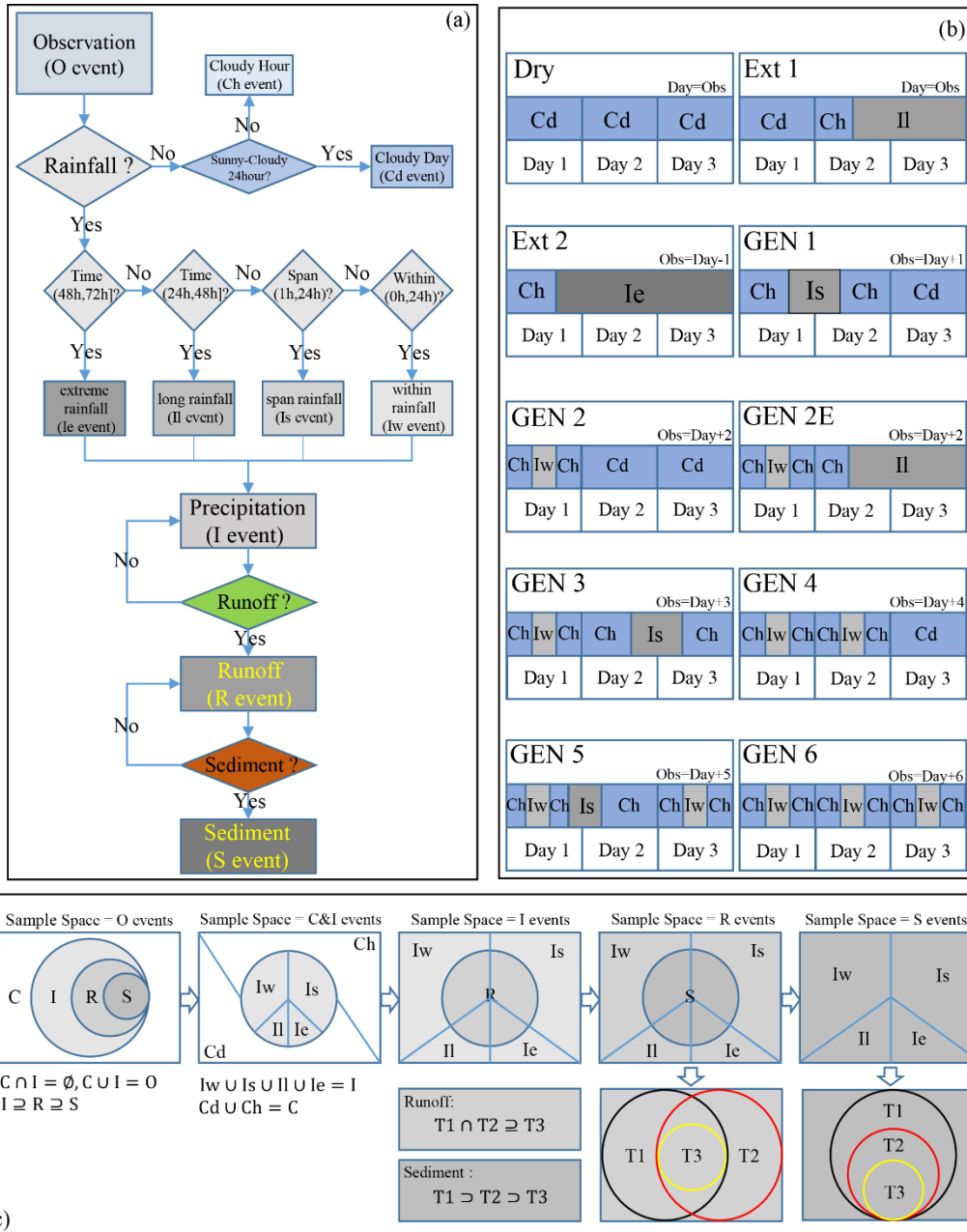


Figure 1 The construction of OCIRS system : (a) a flow chart to determine all random event types in OCIRS framework; (b) the different combining patterns of rainfall and non-rainfall events in three consecutive days to form ten observed random event sequences on five rainy seasons; (c) Venn diagram to reveal the relationship among all random events types in OCIRS framework.

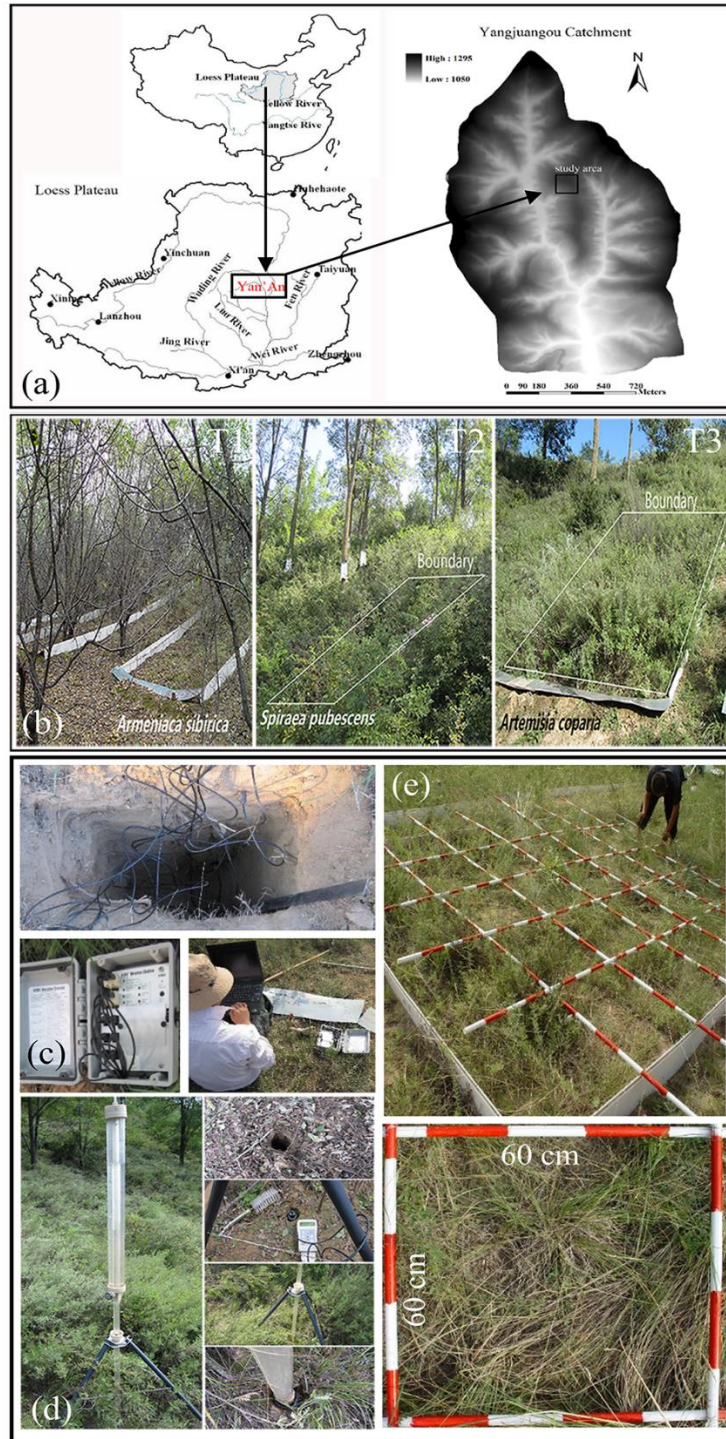


Figure 2 Study area and experimental design: (a) location of the Yangjuangou Catchment; (b) three restoration vegetation types including *Armeniaca sibirica* (T1), *Spiraea pubescens* (T2), and *Artemisia copria* (T3); (c) the dynamic measurement of soil moisture and data collection to provide the information about average antecedent soil moisture; (d) the measurement of field saturated hydraulic conductivity to determine the average infiltration capability; (e): the investigation of morphological properties of restoration vegetation by setting quadrats

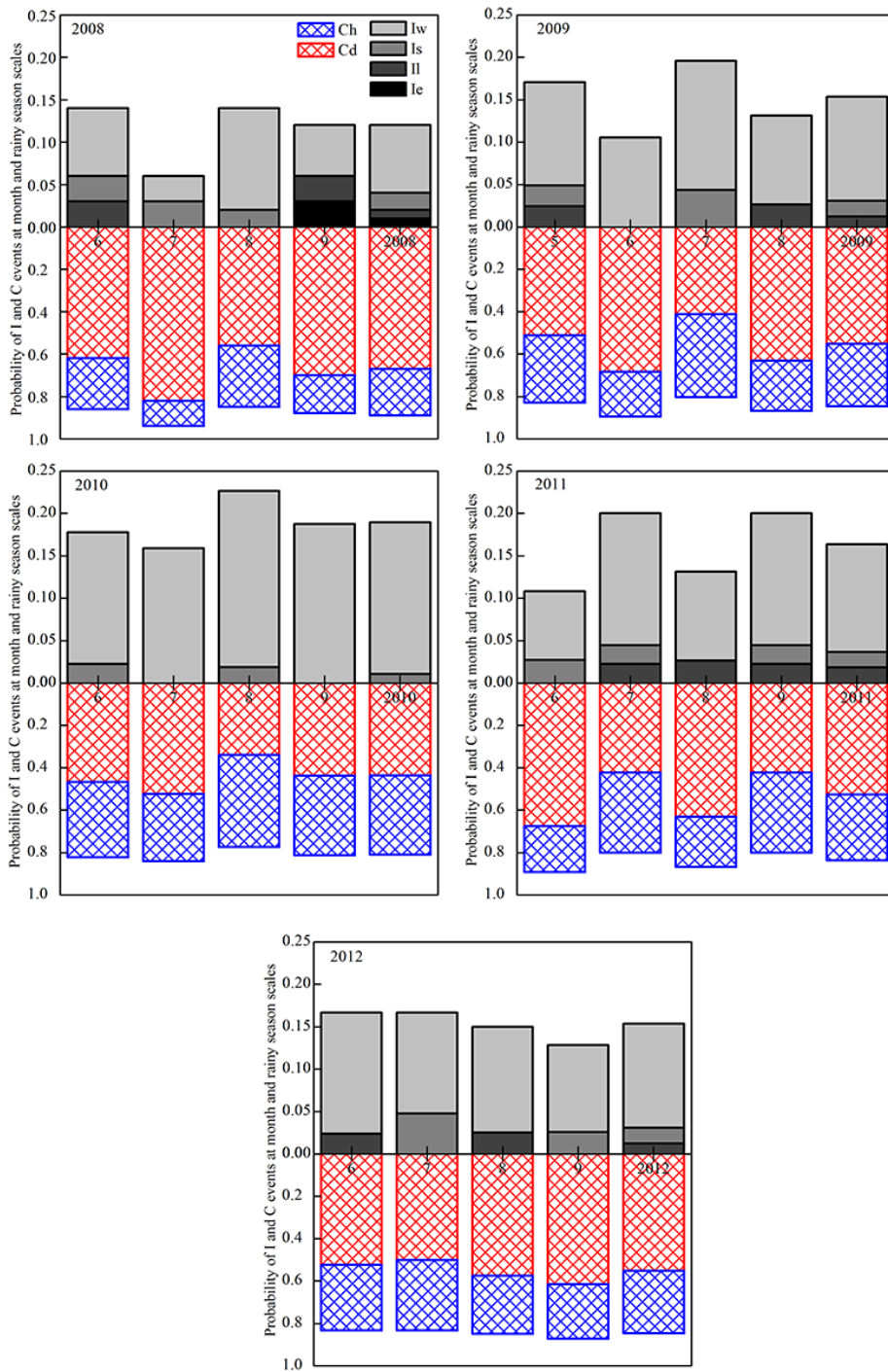


Figure 3 The probability distribution of different random rainfall event types (Iw, Is, Il, and Ie) and random non-rainfall event types (Ch and Cd) at monthly and seasonal scales from rainy season of 2008 to 2012.

1172

1173

1174

1175

1176

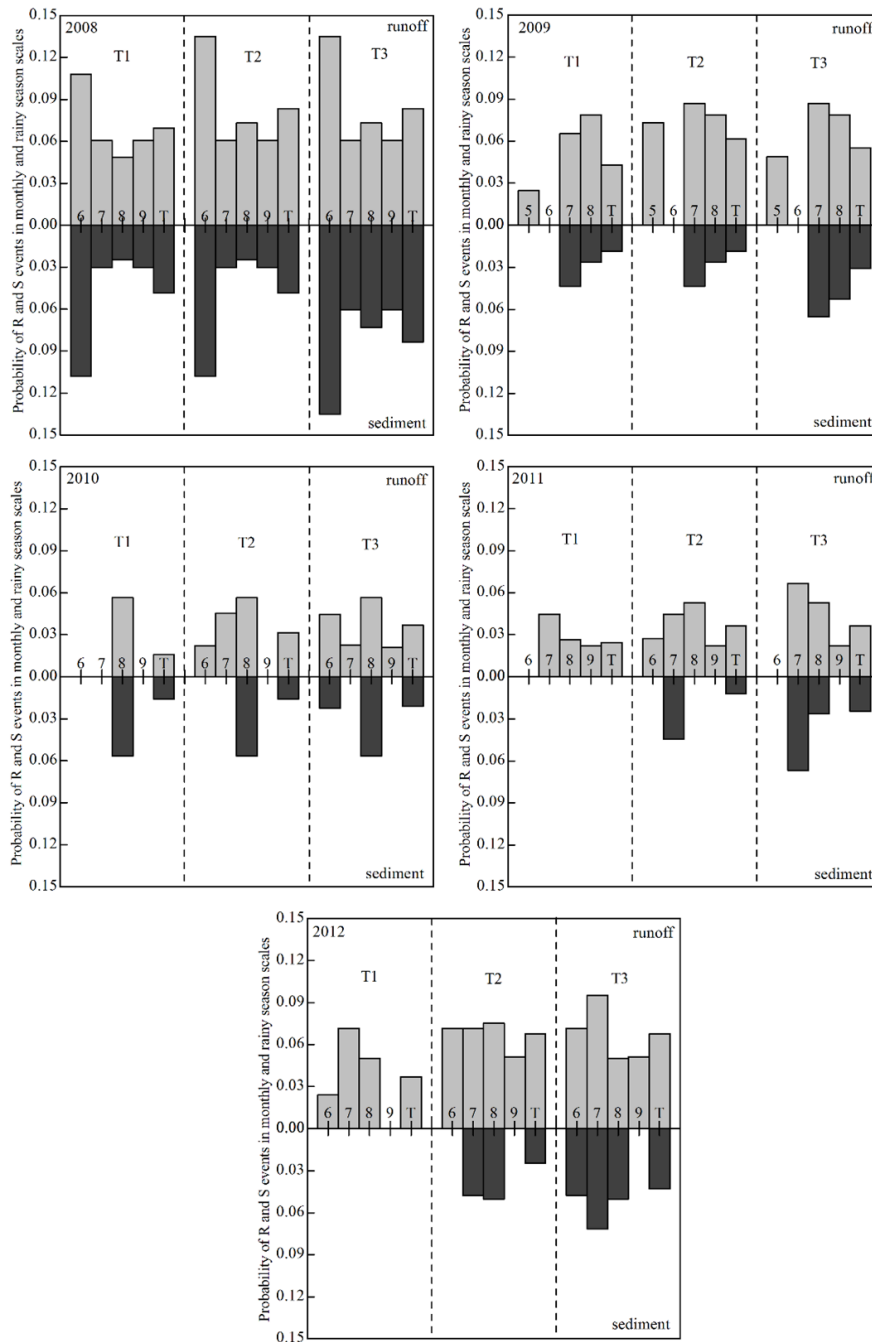


Figure 4 The probability distribution of random runoff and sediment events generating in three restoration vegetation types at monthly and seasonal scales from rainy season of 2008 to 2012, the Arabic numbers and letter “T” on the abscissa indicate the month and season respectively, the same as follow figures

1177
 1178
 1179
 1180
 1181
 1182

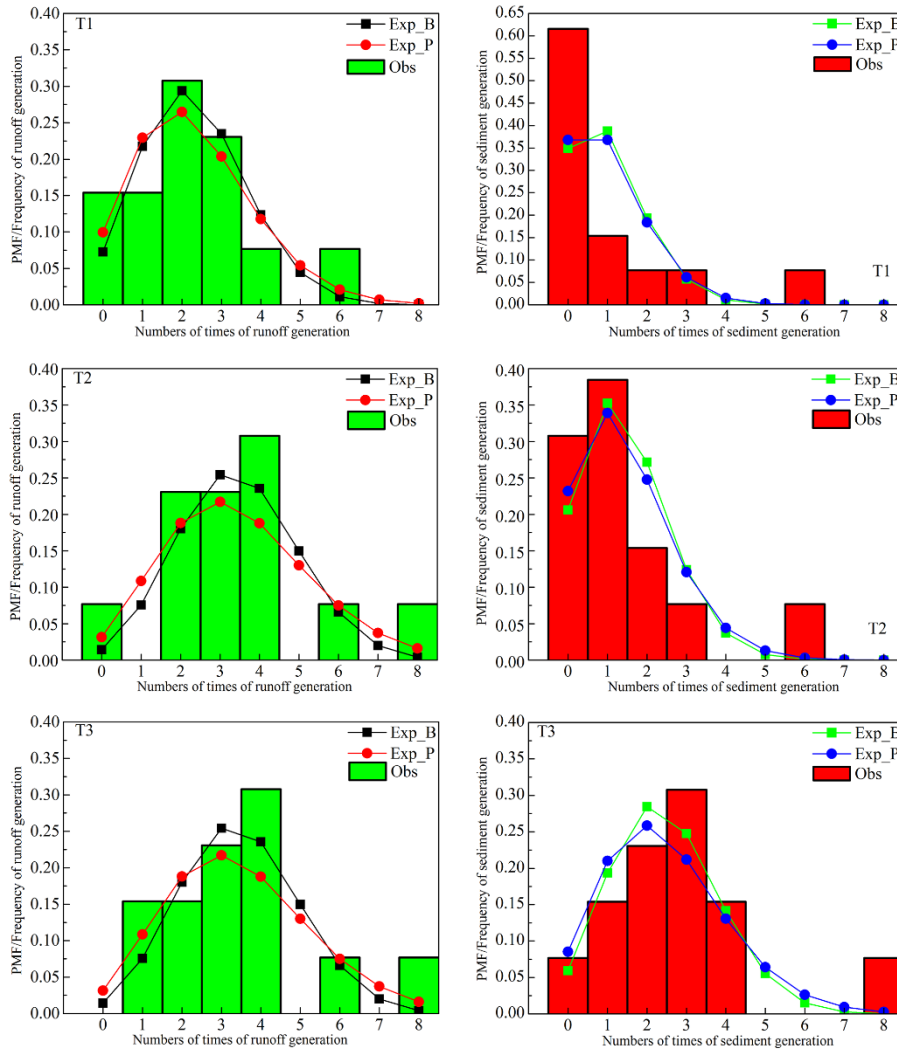


Figure 5 The comparison between simulation of stochasticity of runoff and sediment events by Binomial and Poisson PMFs and the observed frequencies of numbers of times of soil erosion events in three restoration vegetation type, Exp_B and Exp_P indicates the simulated values in Binomial and Poisson PMF respectively, and the histogram represents the observed values.

1183
 1184
 1185
 1186
 1187
 1188
 1189
 1190
 1191
 1192
 1193
 1194
 1195
 1196

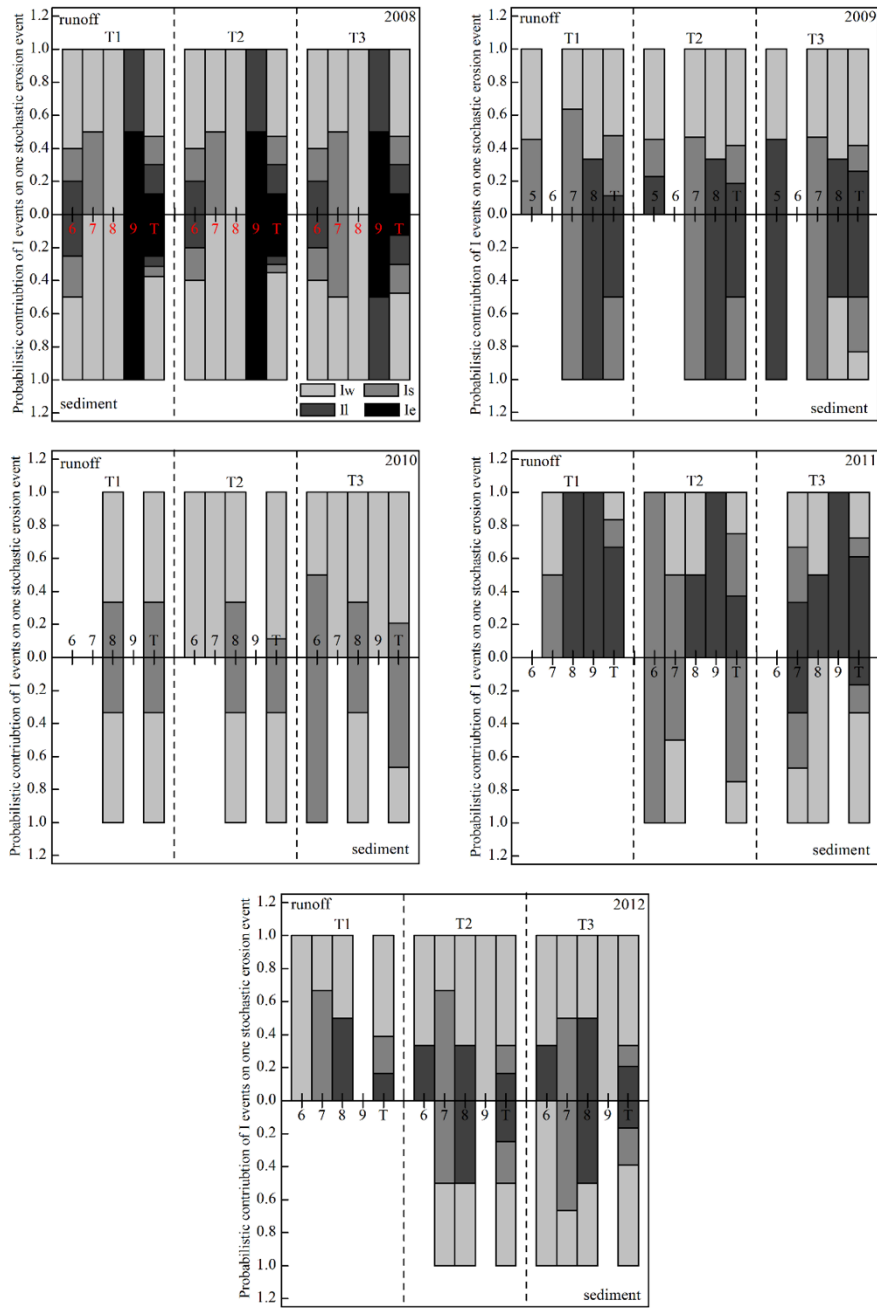


Figure 6 The distribution of probabilistic contribution of four random rainfall event types on anyone runoff or sediment event stochastically generating in three restoration vegetation types at monthly and seasonal scales from rainy season of 2008 to 2012

1197
 1198
 1199
 1200
 1201
 1202
 1203

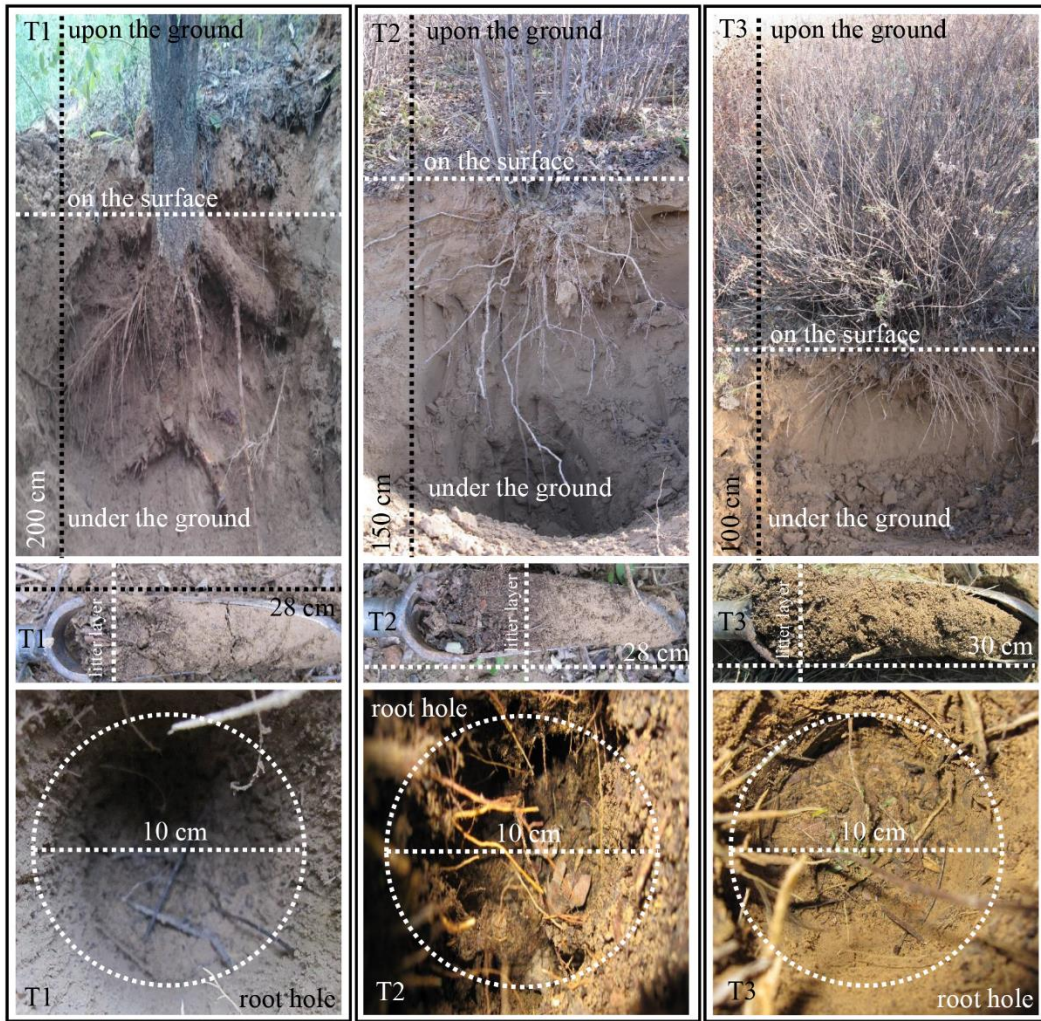


Figure 7 Morphological properties of three restoration vegetation types including the thickness of litter layer, the distribution of root system. The dashed lines indicates the diameter and depth of soil samples with approximating 10 cm and 30 cm respectively.

1204
 1205
 1206
 1207
 1208
 1209
 1210
 1211
 1212
 1213
 1214
 1215
 1216
 1217
 1218

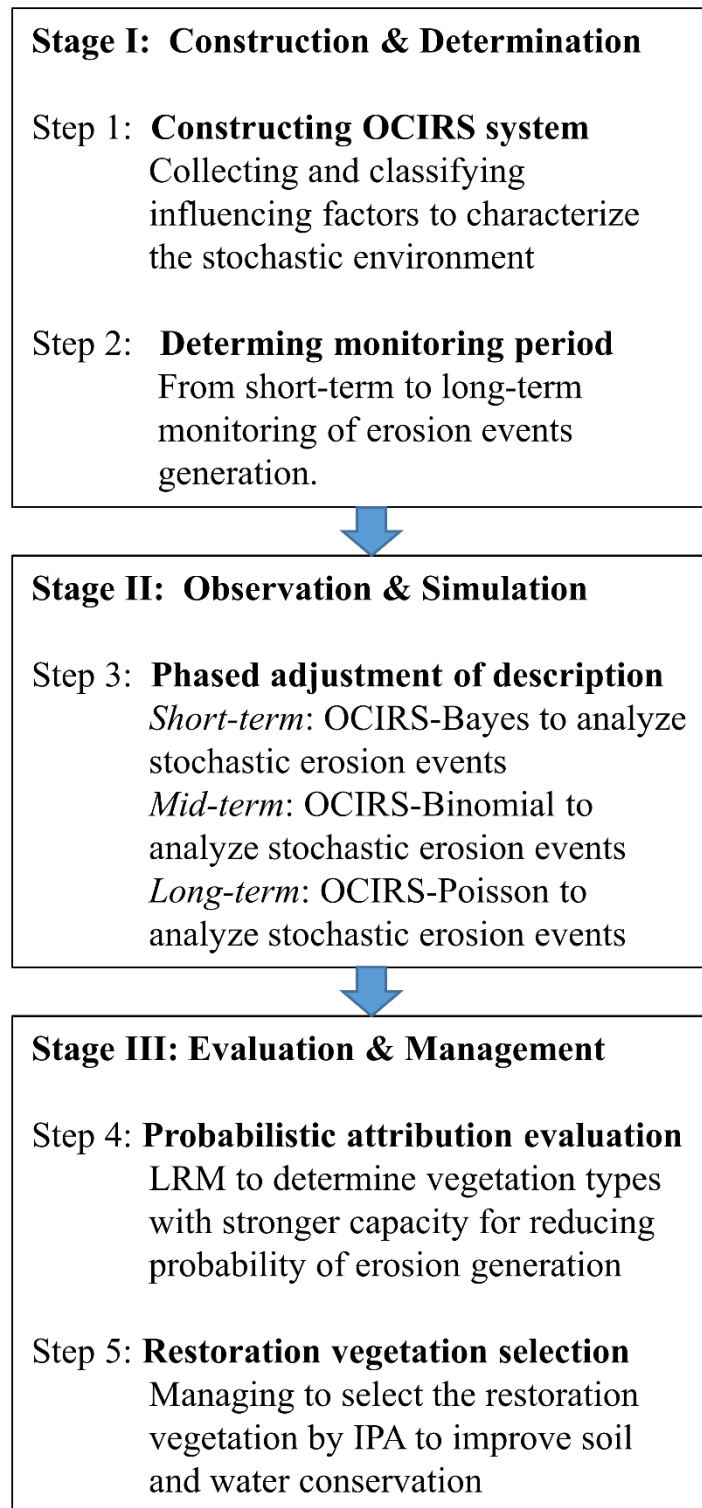


Figure 8 The framework of integrated probabilistic assessment for soil erosion monitoring and restoration strategies

1219
1220
1221
1222